JVI
Journals.ASM.org

Biological Characterization and Next-Generation Genome Sequencing of the Unclassified Cotia Virus SPAn232 (*Poxviridae*)

Priscila P. Afonso,[a] Patrícia M. Silva,[a] Laila C. Schnellrath,[a] Desyreé M. Jesus,[a] Jianhong Hu,[c] Yajie Yang,[c] Rolf Renne,[c] Marcia Attias,[b] Richard C. Condit,[c] Nissin Moussatché,[c] and Clarissa R. Damaso[a]

Laboratório de Biologia Molecular de Vírus[a] and Laboratório de Ultraestrutura Hertha Meyer,[b] Instituto de Biofísica Carlos Chagas Filho, Universidade Federal do Rio de Janeiro, Rio de Janeiro, Brazil, and Department of Molecular Genetics and Microbiology, University of Florida, Gainesville, Florida, USA[c]

Cotia virus (COTV) SPAn232 was isolated in 1961 from sentinel mice at Cotia field station, São Paulo, Brazil. Attempts to classify COTV within a recognized genus of the *Poxviridae* have generated contradictory findings. Studies by different researchers suggested some similarity to myxoma virus and swinepox virus, whereas another investigation characterized COTV SPAn232 as a vaccinia virus strain. Because of the lack of consensus, we have conducted an independent biological and molecular characterization of COTV. Virus growth curves reached maximum yields at approximately 24 to 48 h and were accompanied by virus DNA replication and a characteristic early/late pattern of viral protein synthesis. Interestingly, COTV did not induce detectable cytopathic effects in BSC-40 cells until 4 days postinfection and generated viral plaques only after 8 days. We determined the complete genomic sequence of COTV by using a combination of the next-generation DNA sequencing technologies 454 and Illumina. A unique contiguous sequence of 185,139 bp containing 185 genes, including the 90 genes conserved in all chordopoxviruses, was obtained. COTV has an interesting panel of open reading frames (ORFs) related to the evasion of host defense, including two novel genes encoding C-C chemokine-like proteins, each present in duplicate copies. Phylogenetic analysis revealed the highest amino acid identity scores with *Cervidpoxvirus*, *Capripoxvirus*, *Suipoxvirus*, *Leporipoxvirus*, and *Yatapoxvirus*. However, COTV grouped as an independent branch within this clade, which clearly excluded its classification as an *Orthopoxvirus*. Therefore, our data suggest that COTV could represent a new poxvirus genus.

Poxviruses are brick-shaped viruses with a DNA-containing biconcave core surrounded by one or more envelopes (17). The nine genera within the subfamily *Chordopoxvirinae* are distinguished partially by the different host ranges and geographic distributions of their members but mainly by absent or diminished immune cross-reaction. On the other hand, members of the same genus are genetically related and show strong cross-neutralization (27). During the past 2 decades, the genome sequences of several poxviruses have been elucidated, shedding light on the phylogenetic relationships among family members and providing a genetic basis for classification within distinct genera (1–6, 11, 14, 15, 30, 31, 34, 38, 39, 41, 56, 64, 65, 71). Although most known poxviruses have been grouped within a recognized genus, a few isolates remain unclassified. Unclassified poxviruses include crocodilepox virus, which infects Nile crocodiles (2), squirrelpox virus, which infects squirrels (46), the recently characterized Yoka poxvirus, isolated from mosquitoes in Africa (71), and Cotia virus (COTV), isolated in Brazil (28, 66, 67).

COTV was isolated from 1961 to 1963 from sentinel suckling mice in Cotia field station, São Paulo, Brazil, during an arbovirus surveillance program coordinated by the Instituto Adolfo Lutz, São Paulo (42). The first isolate collected, on 3 March 1961, was designated strain SPAn232 and has been referred to as the COTV prototype (L. E. Pereira and T. L. Coimbra, Section of Arthropod-Transmitted Viruses, personal communication). Strain SPAn232 has not been reisolated, and the natural host for COTV remains unknown. Based on current reports, the assignment of COTV SPAn232 to a recognized poxvirus genus is still controversial. Antibodies against COTV were not able to neutralize infection by vaccinia virus (VACV), myxoma virus (MYXV), goatpox virus (GTPV), or tanapox virus (TANV), suggesting that COTV could not be classified within any poxvirus genus known in the 1970s (66). Further serological tests and analysis of viral proteins showed some similarity between COTV and leporipoxviruses, such as MYXV, but a unique restriction endonuclease profile was reported for the COTV genome (28). In 1995, Ueda and coworkers reported the relatedness of COTV to swinepox virus (SWPV) (*Suipoxvirus*) based on the physical map of the COTV genome and the nucleotide sequence of the thymidine kinase (TK) gene (J2R ortholog in VACV strain Copenhagen [VACV-Cop]) (67). In contrast, later studies based mainly on the sequences of the TK and vaccinia virus growth factor (VGF) (C11R ortholog in VACV-Cop) genes characterized COTV SPAn232 as a VACV strain, which was renamed SAV (19). Further studies confirmed the phylogenetic relationship between SAV and VACV strain WR (24).

Beyond these conflicting results, no information regarding the COTV replicative cycle is available. In this work, we have analyzed the biology and genomics of COTV. Our results show that cultured cells infected with COTV reached a maximum of virus production within 24 to 48 h after infection. Viral proteins and DNA accumulated progressively within this period of infection. Nevertheless, the detection of a typical poxvirus cytopathic effect (CPE), as well as virus plaque formation, was delayed compared to that with VACV infection. We have also determined the complete genomic sequence of COTV by using two high-throughput sequencing strategies, revealing a 185,139-bp genome containing

Received 19 December 2011 **Accepted** 7 February 2012
Published ahead of print 15 February 2012
Address correspondence to Clarissa R. Damaso, damasoc@biof.ufrj.br.

doi:10.1128/JVI.07162-11

185 open reading frames (ORFs). COTV has an interesting set of genes related to immunomodulatory functions, including novel ORFs absent in other poxviruses. Phylogenetic analysis of the 90 proteins conserved in all *Chordopoxvirinae* revealed >65% amino acid identity scores with members of the *Capripoxvirus*, *Suipoxvirus*, and *Cervidpoxvirus* genera. Despite this relatedness, COTV grouped as a distinct branch, suggesting that it probably represents a member of a novel poxvirus genus.

MATERIALS AND METHODS

Cells and viruses. BSC-40 (African green monkey kidney), Vero (African green monkey kidney), Hep-2 (human cervical carcinoma [HeLa contaminant]), C6 (rat glioma), RK-13 (rabbit kidney), L-929 (mouse fibroblast), MEF (mouse embryo fibroblast), CEF (chicken embryo fibroblast), PK-15 (pig kidney), Rat-2 (rat fibroblast), and LLC-MK2 (rhesus monkey kidney) cells were propagated at 37°C in Dulbecco modified Eagle's medium (DMEM; Invitrogen, Carlsbad, CA) supplemented with 5% heat-inactivated fetal bovine serum (Invitrogen), 500 U/ml penicillin, 100 μg/ml streptomycin, 1 mM sodium pyruvate, 2.5 μg/ml amphotericin B (Fungizone), and 0.1 mM nonessential amino acids.

Frozen suckling mice infected with COTV SPAn232 (passage 35 from 19 October 1987) were kindly provided to our laboratory in 1998 by Akemi Suzuki (Instituto Adolfo Lutz, São Paulo, Brazil). Brains were homogenized in phosphate-buffered saline (PBS) supplemented with 1,000 U/ml penicillin, 200 μg/ml streptomycin, and 100 μg/ml gentamicin and were clarified by centrifugation at 600 × *g* for 10 min at 4°C; the supernatant was then used to inoculate BSC-40 cells. The crude stock was subsequently passaged four times, in Vero cells, BSC-40 cells, chorioallantoic membrane (CAM), and BSC-40 cells, and was then subjected to three cycles of plaque purification in BSC-40 cells.

Vaccinia virus (VACV) strain WR was propagated in BSC-40 cells as described elsewhere (22). Myxoma virus (strain Lausanne) and swinepox virus (strain Kasza) were kindly provided by Richard Moyer (University of Florida, Gainesville) and were propagated in RK-13 and PK-15 cells, respectively. Intracellular VACV and COTV were purified from lysates of infected cells by high-speed centrifugation through a 36% sucrose cushion, followed by sedimentation in 25 to 40% sucrose gradients, as described previously (22).

COTV infection and determination of the yield. All infection assays were carried out at 34°C using semiconfluent monolayers infected at a multiplicity of infection (MOI) of 1. After 1 h (adsorption period), the inocula were removed and were replaced with fresh medium for the times indicated in the figure and table legends. Virus yield was determined by a plaque assay in semiconfluent BSC-40 monolayers, and viral plaques were visualized after 9 to 10 days at 34°C following 0.1% crystal violet staining.

Transmission electron microscopy. C6 and BSC-40 cells were infected with COTV for 24 h or 96 h and were processed for transmission electron microscopy analysis as described by Damaso et al. (20). Monolayers were fixed with 2.5% glutaraldehyde in 0.1 M sodium cacodylate buffer (pH 7.2) and were postfixed in 1% osmium tetroxide. Ultrathin sections of the Epon-embedded material were stained using uranyl acetate and lead citrate and were observed using a Zeiss 900 (at the Instituto de Biofísica Carlos Chagas Filho, Universidade Federal do Rio de Janeiro [IBCCF-UFRJ]) or Morgagni 268 (FEI) (at the Instituto de Microbiologia Prof. Paulo de Góes, UFRJ) electron microscope.

Analysis of COTV DNA replication. BSC-40 and C6 cells in 35-mm-diameter dishes were infected with COTV as described above. Viral DNA accumulation was investigated essentially as described previously (21, 52). Briefly, at various times postinfection, cells were harvested in TLD buffer (10× SSC [1.5 M NaCl, 0.15 M sodium citrate] [pH 7.0], 1 M ammonium acetate), and samples (40 μl) were applied in triplicate to nylon membranes for slot blot DNA hybridization. COTV DNA isolated from purified virions and radiolabeled by nick translation was used as a probe (21). Densitometry analysis of the X-ray films was performed using Scion Image (beta release 4; Scion Corporation).

Analysis of viral proteins. (i) [^{35}S]methionine incorporation. BSC-40 and C6 cells in 35-mm-diameter dishes were infected with COTV. At multiple times of infection, cells were pulse-labeled for 1 h with 80 μCi/ml [^{35}S]methionine-[^{35}S]cysteine (Perkin-Elmer Life Sciences) in methionine-free medium (Invitrogen). Cells were then harvested in sodium dodecyl sulfate (SDS) sample buffer, and samples were subjected to electrophoresis in a 12% SDS-polyacrylamide gel electrophoresis (PAGE) gel, as described previously (22). The gels were dried and exposed to X-ray films.

(ii) Detection of viral proteins by immunoblotting. A hyperimmune antiserum against COTV proteins was obtained by inoculating two male rabbits with SDS-solubilized proteins of purified COTV, as described elsewhere for anti-VACV serum preparation (21). A rabbit anti-MYXV serum was kindly provided by Grant McFadden (University of Florida, Gainesville). For Western blot assays, BSC-40 cells were infected with COTV or VACV-WR. PK-15 or RK-13 cells were infected with SWPV or MYXV, respectively. At the times of infection indicated in the figure legends, samples were processed for SDS-PAGE, followed by Western blotting essentially as described by Damaso et al. (20). Primary antibody dilutions were 1:2,000 for 1 h (anti-VACV and anti-COTV) and 18 h (anti-MYXV). Viral proteins were detected by incubation with rabbit anti-IgG conjugated to horseradish peroxidase, followed by Western blotting Luminol reagent (Santa Cruz Biotechnology, Santa Cruz, CA).

(iii) Detection of viral proteins by immunofluorescence assay. BSC-40 and C6 cells were grown in 13-mm-diameter round glass coverslips in 24-well plates and were infected with COTV at an MOI of 1. After 48 h, the monolayers were fixed in 4% paraformaldehyde-PBS, permeabilized using 0.5% Triton X-100 as described previously (16), and stained with anti-COTV for 1 h, followed by Alexa 488-conjugated rabbit anti-IgG (Invitrogen). DNA was detected by staining with 4′,6-diamidino-2-phenylindole (DAPI). Samples were analyzed with a Zeiss Axio Observer Z1 inverted microscope, and confocal images were acquired with a Zeiss LSM 510 META confocal microscope.

Genomic library construction and DNA sequencing. COTV genomic DNA was isolated from purified particles by using the DNeasy Blood & Tissue kit (Qiagen, Valencia, CA) as suggested by the manufacturer and was subjected to high-throughput sequencing using the Genome Sequencer FLX (454 Life Sciences, Branford, CT) and Genome Analyzer IIx (Illumina, San Diego, CA) at the Interdisciplinary Center for Biotechnology Research (ICBR), University of Florida. Sanger sequencing was also performed for confirmatory purposes and for DNA walking on genome ends at ICBR and at the Unidade Multidisciplinar de Genômica (Instituto de Biofísica Carlos Chagas Filho, UFRJ). In preparation for 454 sequencing, a single-strand template DNA (sstDNA) library was constructed using a GS FLX Titanium general library preparation kit and was amplified by emulsion PCR (emPCR) using the GS FLX Titanium SV and LV emPCR kits. A picotiter plate with the beads was loaded onto a 454 instrument along with the reagents, and sequences were obtained according to the manufacturer's protocol. For Illumina sequencing, COTV DNA was sheared using sonication and was blunt ended with T4 DNA polymerase and Klenow DNA polymerase. After the ligation of adapters to both ends, DNA fragments within the range of 250 to 400 bp were gel purified and PCR amplified with 18 cycles. The resulting libraries were gel purified and were quantified using the KAPA Library Quant Kit (Kapa Biosystems) on an ABI 7900HT real-time PCR system. Libraries were diluted to 10 pM for cluster generation on cBOT. The 2 × 100 cycle paired-end sequencing run was performed on an Illumina GA platform (running SCS 2.8) using a single lane of an 8-lane flow cell according to the manufacturer's instructions.

Sequence assembly, genome analysis, and phylogenetic inference. An initial assembly of the 454 sequences was performed with the Newbler assembler, version 2.3 (454 Life Sciences), with masking and trimming sequencing repeats, primers, and/or adapters used in sequencing library preparation and normalization. Illumina data were assembled *de novo* using Velvet with a *k*-mer of 55 and a short paired insert length of 225 (70), after removal of adapters using fastx_clipper (FASTX-Toolkit, version

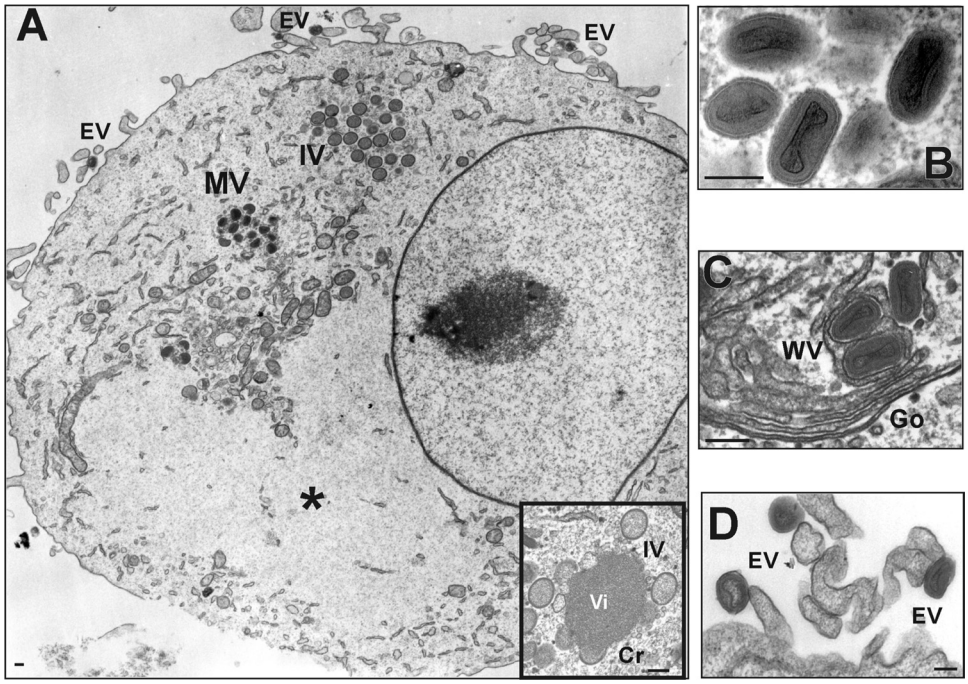

FIG 1 Electron microscopy analysis of COTV-infected cells. C6 (A, B, and D) and BSC-40 (C) cells were infected with COTV at an MOI of 1. The monolayers were fixed and processed for transmission electron microscopy at 24 h (A) or 96 h (B to D) postinfection. Representative fields are shown. (A) Mature viruses (MV) and immature spherical particles (IV) are visualized in the cytoplasm outside areas devoid of cellular organelles resembling Cotia bodies (asterisks). Extracellular viruses (EV) are found associated with the cell membrane. (Inset) High-magnification image of viroplasm (Vi) surrounded by membrane crescents (Cr) and IV. (B) High-magnification image of MV. (C) MV are enveloped by additional membranes derived from the *trans*-Golgi complex, generating wrapped virions (WV). The Golgi apparatus (Go) is shown. (D) High-magnification image of EVs associated with the cell membrane. Bars, 200 nm.

0.0.6). Any orphan reads were removed using an in-house Perl script. Combined assembly of 454 and Illumina contigs together with Sanger reads resulting from walking on the genome was performed using SeqMan (DNAStar package; Lasergene Inc.), with default parameters. Open reading frames (ORFs) longer than 30 amino acids were detected by FGENESV (Softberry), Vector NTI (Invitrogen), and CLC DNA Workbench (CLC bio, Aarhus, Denmark). Predicted ORFs containing poxvirus promoter elements and/or transcription termination signals were annotated. A total of 185 ORFs were identified by a homology search using BLASTP, available through the NCBI website (http://blast.ncbi.nlm.nih.gov/Blast.cgi). Tandem repeats were identified by Tandem Repeat Finder (12).

Phylogeny inference was performed by aligning the predicted amino acid sequences obtained for each of the 90 conserved genes with ortholog sequences from 21 different chordopoxviruses by use of Clustal X, version 1.81 (60), and MUSCLE, version 3.8 (25). After visual inspection of the alignments, the external gaps were excluded, and a concatenated data set was obtained by combining the alignments for each gene into a single alignment of 30,717 amino acids. All sequence manipulation steps were carried out twice as independent events. The combined data sets were used to generate neighbor-joining phylogenetic trees using MEGA, version 4 (59), opting for the JTT model of substitution, and 2,500 bootstrap replicates. Alternatively, maximum-likelihood trees were inferred using Puzzle, version 5.2 (54), opting for the WAG correction for multiple substitutions, a neighbor-joining input tree, 10,000 quartet puzzling steps, and an eight-category discrete gamma model. DNA sequences were aligned using KALIGN (37) and were adjusted by visual inspection.

The GenBank accession numbers of the poxvirus DNA genome sequences used for the multiple alignments were as follows: canarypox virus (CNPV) strain ATCC VR111, NC_005309; fowlpox virus (FWPV) strain Iowa, NC_002188; deerpox virus (DPV) strains W-848-83 and W-1170-84, NC_006966 and AY689437; swinepox virus strain Nebraska, NC_003389; myxoma virus strain Lausanne, NC_001132; rabbit fibroma virus (RFV) strain Kasza, NC_001266; goatpox virus strain Pellor, NC_004003; lumpy skin disease virus (LSDV) strain Neethling Warmbaths, AF409137; sheeppox virus (SPPV) strain Niskhi, AY077834; Yaba-like disease virus (YLDV) strain Davis, NC_002642; Yaba monkey tumor virus (YMTV) strain Amano, NC_005179; cowpox virus (CPXV) strain Brighton Red, NC_003663; monkeypox virus (MPXV) strain Liberia_1970_184, DQ011156; vaccinia virus strain WR (VACV-WR), NC_006998; vaccinia virus strain Copenhagen (VACV-Cop), M35027; variola minor virus (VARV) strain Garcia, Y16780; molluscum contagiosum virus (MOCV), NC_001731; bovine papular stomatitis virus (BPSV), NC_005337; orf virus (ORFV) strain NZ2, DQ184476; and crocodilepox virus (CRV) strain Zimbabwe, NC_008030.

Nucleotide sequence accession number. The COTV genome sequence has been deposited in GenBank under accession number HQ647181.

RESULTS

Virus morphology and host range. After the isolation of COTV SPAn232 from sentinel mice in 1961, the Instituto Adolfo Lutz propagated virus samples only by sequential intracranial passage of brain suspensions in 3-day-old mice. The last passage dates from 5 May 2003 and was derived from passage 34, which was used to generate passage 35 in two independent inoculation events: in 1987 and 2003 (T. L. Coimbra, personal communication). Passage 35 from 1987 was sent to our laboratory in 1998.

After adaptation to cell culture and three consecutive cycles of plaque purification, crude stocks of COTV were prepared and were used to infect C6 and BSC-40 cells in order to evaluate virus morphogenesis and to confirm the typical poxvirus morphology of the isolate. We observed all stages of poxvirus morphogenesis in

TABLE 1 Production of COTV progeny in different cell types[a]

Cell line (species)	PFU per cell
BSC-40 *(Cercopithecus aethiops)*	20 ± 3
C6 *(Rattus norvegicus)*	17 ± 1
RK-13 *(Oryctolagus cuniculus)*	9 ± 4
L-929 *(Mus musculus)*	7 ± 4
Hep-2 *(Homo sapiens)*	7 ± 1
MEF *(Mus musculus)*	5 ± 4
Vero (*Cercopithecus aethiops)*	4 ± 2
CEF *(Gallus gallus domesticus)*	2 ± 2
PK-15 *(Sus scrofa)*	0
LLC-MK2 (*Macaca mulatta)*	0
Rat-2 *(Rattus norvegicus)*	0

[a] Cells were infected with COTV at an MOI of 1 and were collected at 52 h postinfection for virus titration by plaque assay in BSC-40 cells, as described in Materials and Methods. Results are means (± standard deviations) for three assays titrated in duplicate.

the cell cytoplasm (Fig. 1): crescents (Cr), spherical immature particles (IV), mature particles (MV), wrapped virus (WV), and extracellular virus (EV). Inclusions devoid of cellular organelles similar to the granular Cotia bodies described by Ueda et al. (66) were also visualized (Fig. 1A, asterisk). These inclusions were less electron dense than typical viroplasm (Fig. 1A, inset).

The production of COTV progeny during the infection of several cell types was analyzed 52 h postinfection by a plaque assay in BSC-40 cells (Table 1). We observed that distinct cell types produced similar virus yields, but C6 and BSC-40 cells generated higher titers than other cell types. In PK-15, LLC-MK2, and Rat-2 cells, specifically, progeny production was negligible. It is worth noting that all cell types tested in this assay were fully permissive to VACV (data not shown).

During the course of these assays, we observed that COTV generated tiny plaques detectable only after 8 days of infection. Plaque formation was dependent on monolayer confluence and incubation temperatures of 33°C to 34.5°C. Figure 2A shows the COTV plaque phenotype in BSC-40 cells at 9 days postinfection. Plaques were significantly smaller than VACV-WR plaques visualized at 48 h postinfection. We have also observed that the virus-induced cytopathic effect (CPE) progressed quite slowly in BSC-40 cells compared with that in C6 cells infected with COTV. Figure 2B shows that no apparent CPE was detected in BSC-40 cells at 48 h postinfection, while in C6 monolayers, typical cell rounding induced by poxvirus infection could be observed. CPE in BSC-40 cells was noticed only after 4 days of infection at an MOI of 1. In both cell lines, however, these effects proceeded much more slowly than the morphological changes induced by VACV-WR infection (Fig. 2B). It is noteworthy that viral DNA and COTV structural proteins could be detected in BSC-40 monolayers presenting normal cellular morphology, indicating active infection in these cells (Fig. 2C, top). Cells stained with anti-COTV contained viral factories characteristic of late-stage infection (Fig. 2C, center). A similar pattern was observed in C6 cells (Fig. 2C, bottom).

Analysis of the COTV replicative cycle. To further investigate COTV infection in BSC-40 and C6 cells, we analyzed virus progeny production and DNA replication in time course assays. As shown in Fig. 3A, the infection of the two cell lines generated similar kinetics of virus growth, which reached a plateau at approximately 48 h in BSC-40 cells and 24 h in C6 cells. The time course profile of progeny yield in C6 cells was similar to that reported previously for VACV-infected BSC-40 cells, although virus production by VACV is at least 5 times greater than that by COTV (23).

A time course assay of COTV DNA accumulation was evaluated by slot blot hybridization of infected-cell extracts. As shown in Fig. 3B, the viral DNA contents in both cell lines increased with time, reaching a plateau after 24 h of infection. The time course profiles were similar to those observed for progeny production assays, and similar kinetics of DNA accumulation have been observed in VACV-infected cells (23).

We also analyzed viral protein synthesis during the course of infection. BSC-40 and C6 cells infected with COTV were pulse-labeled with [^{35}S]methionine at the time points indicated in Fig. 3C, and samples were resolved by SDS-PAGE, followed by autoradiography. In both cell lines, the analysis revealed the typical pattern of pre- and postreplicative polypeptides observed for other poxviruses (Fig. 3C). Viral early proteins were initially detected at 2 h postinfection (Fig. 3C, arrowheads), followed by the onset of late protein synthesis at 8 h, progressing up to 24 h postinfection (Fig. 3C, circles). Interestingly, although we observed the inhibition of cellular protein synthesis as infection developed (Fig. 3C, asterisks), this effect was not as dramatic as the typical shutoff of host translation observed during infection with VACV (9, 22).

Together, these data indicate that COTV successfully developed all stages of the replicative cycle within 24 h of infection, with equivalent kinetics in C6 and BSC-40 cells, despite the formation of relatively small plaques and the delay in the development of CPE observed in both cell lines. Therefore, these data support the conclusion that COTV is clearly distinct from VACV. In addition, we investigated the immunological relationships of COTV with VACV, MYXV, and SWPV. Western blot analysis of cells infected with COTV, VACV-WR, MYXV, and SWPV revealed that anti-COTV primarily detected several COTV proteins, cross-reacting slightly, but equally, with VACV, MYXV, and SWPV high-molecular weight polypeptides (Fig. 4A, left). Similarly, no significant cross-reactivity was detected with antisera against other viruses (Fig. 4A). In addition, an anti-COTV antiserum failed to neutralize VACV, MYXV, or SWPV infection but efficiently neutralized COTV infection (Fig. 4B). These data suggested that COTV does not belong to the *Orthopoxvirus*, *Leporipoxvirus*, or *Suipoxvirus* genus.

Sequencing and structure of the COTV genome. To proceed with COTV characterization in detail, we determined the complete nucleotide sequence of the COTV genome by using a combination of two high-throughput sequencing strategies, 454 GS-FLX Titanium and Illumina GAII, plus traditional Sanger sequencing (the latter used mainly to primer-walk on the ends of the genome). The 454 sequencing of the COTV genome yielded 41,387 raw reads (average length, 371 nucleotides [nt]), which were assembled into 550 contigs (average length, 1,110 nt). Two contigs of 157,656 nt and 13,281 nt were used for further assembly (average 60× genome coverage). The Illumina sequencing produced 27,415,784 raw read pairs of 105 nt, which were used by the Velvet assembler to generate 6,624 small contigs of variable lengths. The Illumina reads resulted in an average 962× coverage of the COTV genome. Nucleotide mismatches and possible errors in homopolymeric regions of 454 contigs not corrected by Illumina were solved by Sanger

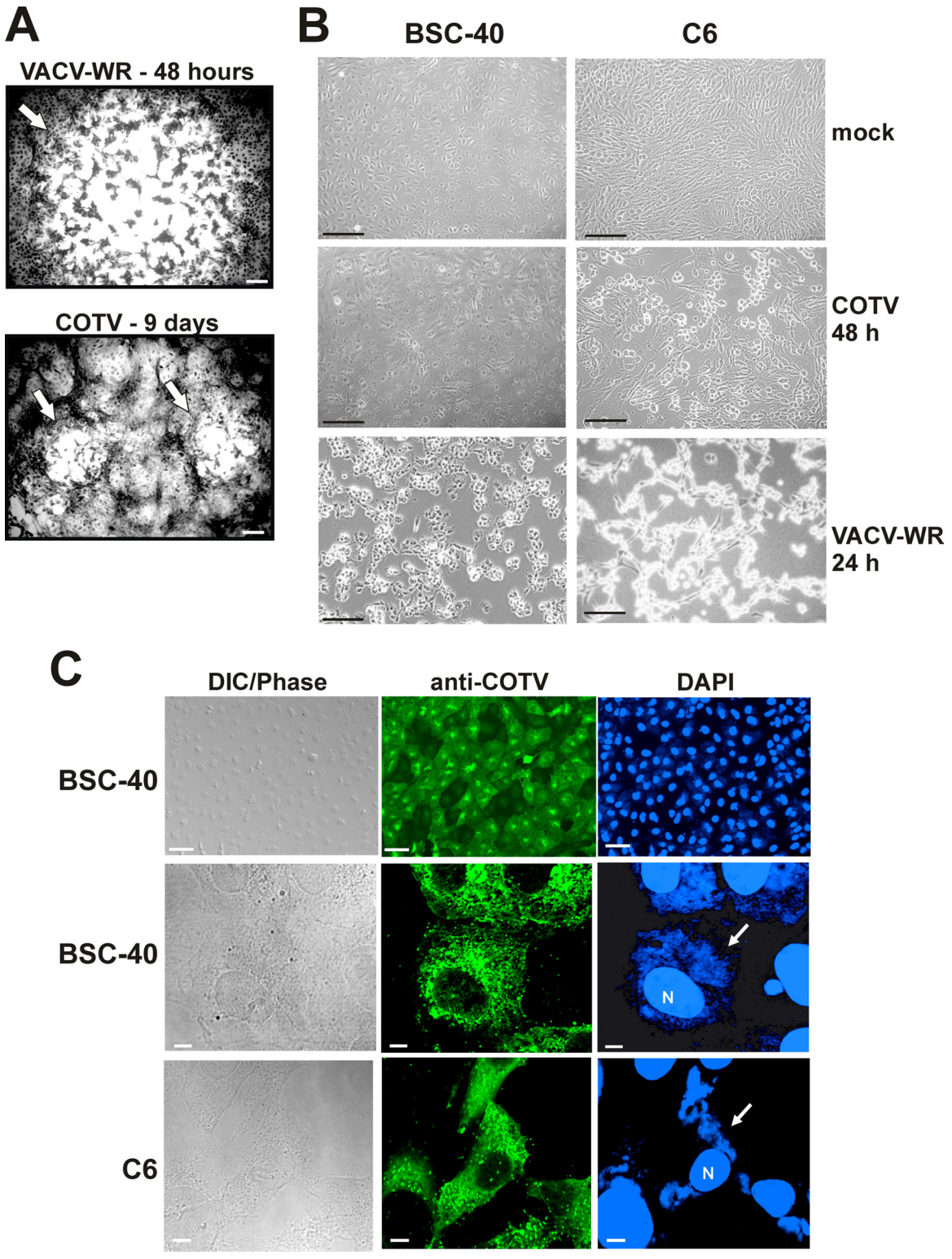

FIG 2 Virus plaque phenotype and CPE progression in COTV-infected cells. (A) Monolayers of BSC-40 cells were infected with 300 PFU of VACV-WR or COTV for 2 or 9 days, respectively, at which time the cells were stained with 0.1% crystal violet. Arrows indicate viral plaques. Bars, 100 μm. (B) BSC-40 and C6 cells were either mock infected or infected with COTV or VACV-WR at an MOI of 1, and CPE was visualized at 24 (VACV-WR) or 48 (COTV) h postinfection. Bars, 100 μm. (C) BSC-40 and C6 cells were infected with COTV at an MOI of 1 for 48 h and were processed for immunofluorescence assays using an antiserum against COTV structural proteins (anti-COTV). DNA was stained with DAPI. N, nucleus. Arrows point to virus factories in the cell cytoplasm. Representative fields are shown. Bars, 50 μm (top) and 5 μm (center and bottom).

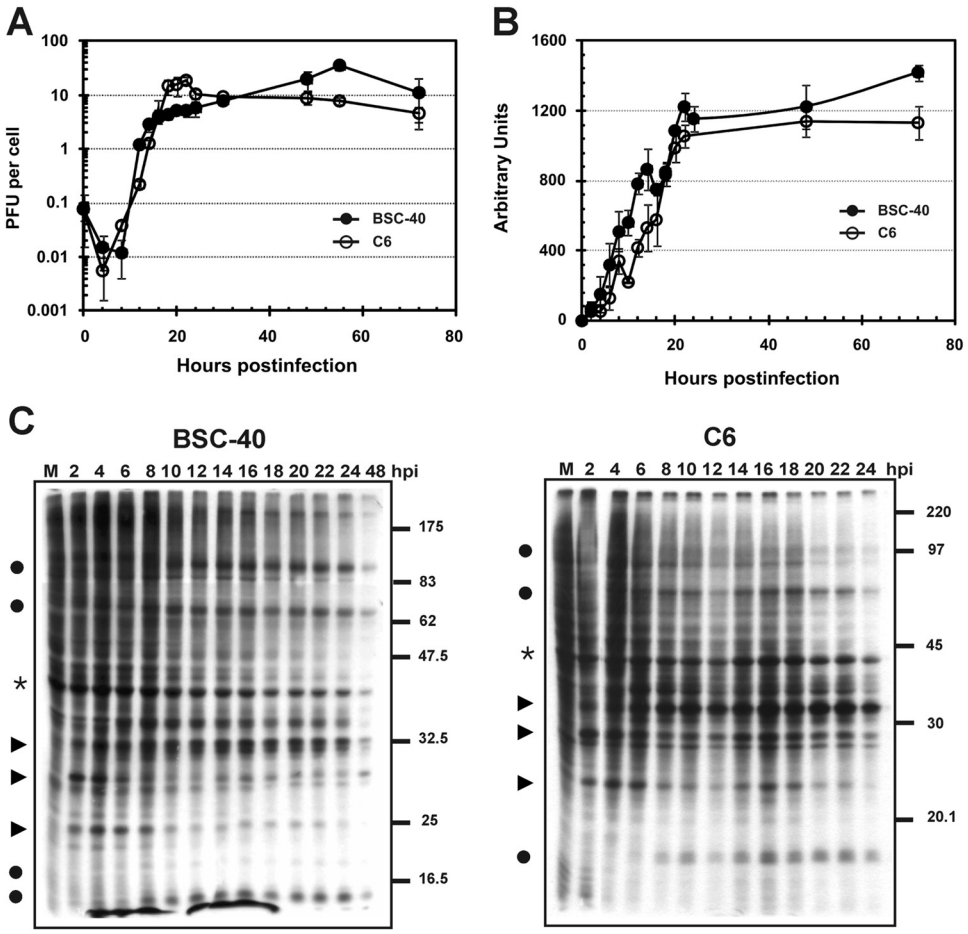

FIG 3 Time course analysis of progeny production, DNA replication, and protein synthesis in COTV-infected cells. Semiconfluent BSC-40 and C6 monolayers were infected with COTV at an MOI of 1, and at the indicated times postinfection, cells were either harvested for virus titration by plaque assay (A), processed for detection of viral DNA by slot blot hybridization (B), or pulse-labeled with [^{35}S]methionine followed by 12% SDS-PAGE analysis (C). (A) Values represent the means for three assays titrated in duplicate. (B) The autoradiograms obtained for BSC-40 and C6 cells were scanned, and densitometry analysis was performed. The numbers (arbitrary units) express the mean values for nine autoradiograms in which samples were applied in triplicate. (C) Representative autoradiograms are shown. Filled circles indicate viral late proteins; arrowheads indicate viral early proteins; asterisks indicate a host protein. M, mock-infected cells. Molecular size markers (in kilodaltons) are given on the right.

sequencing. Assembly of Illumina contigs with the two 454 contigs and the Sanger reads resulting from primer walking on the inverted terminal repeat (ITR) regions generated a final contiguous sequence of 185,139 bp.

The COTV genome has an average A+T content of 76.4% and a central genomic region of 157,703 bp flanked by two identical ITRs of 13,718 bp. The ITR contains 16 copies of a 17-bp tandem repeat and 11 copies of a 24-bp tandem repeat, which are partially inserted into 2 distinct 47-bp tandem repeats present in 6 copies each. These repeats are also present in 2 copies of a 132-bp element. As with other poxviruses, the leftmost nucleotide of the final assembled sequence was arbitrarily set to nucleotide number 1.

COTV contains 185 ORFs, which account for a coding density of 91.5% (Fig. 5; Table 2). Fifteen ORFs are duplicated, with one copy located in each ITR. As with other poxviruses, ORFs situated in the middle region of the COTV genome encode proteins related to viral DNA and RNA metabolism, the structure of virus particles, and virion morphogenesis. Within this region, we identified the 90 conserved genes present in all chordopoxviruses, located between VACV-Cop orthologs F9L and A34R (COTV040 to COTV141). Gene synteny in this region is conserved overall in COTV relative to members of the *Chordopoxvirinae* (Table 2). The ends of the genome encode proteins involved in the modulation of host immune response, virulence, and host range, as well as some proteins of unknown function (Fig. 5).

Notable genes in the COTV genome possibly related to immunomodulation and virulence. COTV has an interesting panel of ORFs possibly related to immunomodulation, virulence, and host range (Table 2; Fig. 5). It encodes 5 serine protease inhibitor (serpin)-like proteins, 6 kelch-like proteins, 4 C-C chemokine binding proteins, 4 C-C chemokine-like proteins, and 13 proteins with ankyrin repeats, 5 of which possess C-terminal PRANC domains (F-box-like domains). COTV also codes for proteins related to the evasion of the interferon (IFN) response, such as protein kinase R (PKR) inhibitors, encoded by COTV029 and COTV051 (orthologs of VACV-Cop K3L and E3L), IFN-γ receptor-like protein (COTV017), and three IFN-α/β receptor-like proteins (COTV009, COTV020, and COTV177). Interestingly, COTV009 and COTV177 are duplicated copies of the same gene

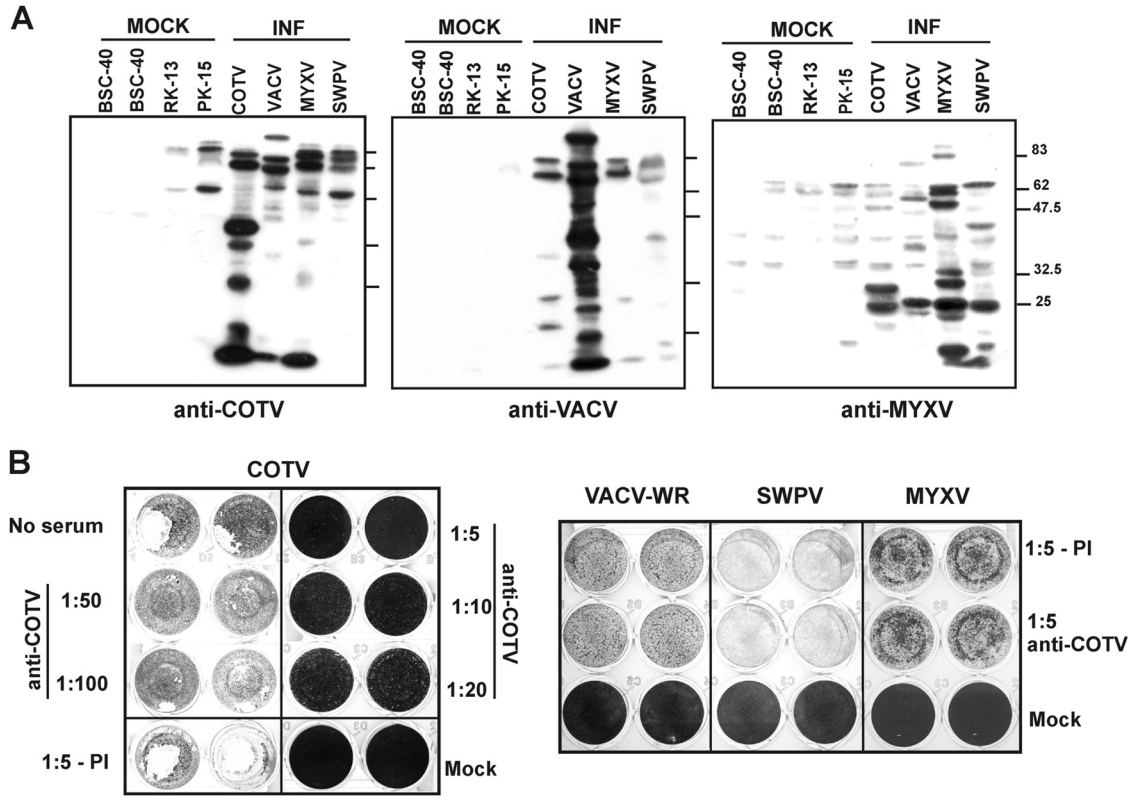

FIG 4 Analysis of COTV cross-reactivity and virus neutralization. (A) The indicated cells were infected (INF) with COTV (BSC-40), VACV (BSC-40), MYXV (RK-13), or SWPV (PK-15) at an MOI of 5 and were harvested after reaching intense CPE (for COTV, 4 days; for VACV, 24 h; for MYXV, 48 h; for SWPV, 3 days). Samples were analyzed by Western blotting using an antiserum against COTV (left), VACV (center), or MYXV (right). (B) A total of 10,000 PFU of COTV, VACV, MYXV, or SWPV was incubated with the indicated dilutions of anti-COTV antiserum or the preimmune serum (PI) for 1 h at 37°C. The mixtures were then placed on monolayers of BSC-40 (COTV and VACV), RK-13 (MYXV), or PK-15 (SWPV) cells for 9 days (COTV) or for 48, 52, or 96 h postinfection (VACV, MYXV, or SWPV, respectively), after which virus-induced CPE was visualized by crystal violet staining.

located in the ITRs, but COTV020 is a different ortholog, sharing 29% amino acid identity with COTV009 and COTV177. Other proteins are complement binding protein (COTV026), major histocompatibility complex class II (MHC-II) inhibitor (COTV142), concanavalin-like precursor (COTV143), CD47-like protein (COTV146), Ig domain OX-2-like protein (COTV153), and MHC-I antigen-like protein (COTV170).

Also present in the COTV genome are genes related to NF-κB inhibition, such as orthologs of VACV-Cop M2L (COTV028), K1L (COTV031), B15R (COTV166 and COTV174), and N1L (COTV156), and ORFs involved in the modulation of apoptosis: COTV034 and COTV165 are predicted to encode orthologs of the apoptosis regulatory protein of YMTV (VACV-Cop F1L) and the serpin CrmA/SPI-2 of CPXV, respectively. We also identified five tumor necrosis factor (TNF) receptor-like proteins: COTV007 and COTV179 (orthologs of CPXV CrmB), COTV008 and COTV178 (orthologs of CPXV CrmE), and COTV168 (ortholog of a CrmB pseudogene of CPXV). Of these, only the orthologs of CrmE have typical TNF-binding domains and are likely to be functional.

Notably, the COTV genome lacks an ortholog of VACV-Cop B5R, which is involved in the wrapping of intracellular MV to generate WV and in the formation of EV (26, 53). Nevertheless, COTV encodes all other proteins involved in these final stages of WV and EV formation, i.e., orthologs of VACV-Cop F12L, F13L, E2L, A33R, A34R, and A36R (COTV043, COTV044, COTV050, COTV140, COTV141, and COTV144), as well as of F11L (COTV042), recently shown to be involved in VACV release (18).

Novel genes unique to the COTV genome. COTV contains 6 genes that are predicted to encode proteins with no homologs within poxviruses (Table 2). COTV021 and COTV045 encode proteins with no significant homology to any sequences currently in the databases. On the other hand, COTV003/COTV183 and CTOV010/COTV176 are duplicated genes located in the ITRs and are predicted to encode C-C chemokine-like proteins of 11.9 kDa and 13.16 kDa, respectively. COTV003/COTV183 are similar to C-C chemokine ligand 13 (CCL13) of the ferret (*Mustela putorius furo*) (BLASTP E value, 9e−06). The predicted COTV protein has a secretory signal peptide, two putative glycosaminoglycan (GAG) binding sites, and one putative receptor-binding site, in addition to other domains characteristic of C-C chemokines, all inserted within the chemokine superfamily domain (Fig. 6). CTOV010/COTV176 are similar to the small inducible cytokine A2 precursor of the rodent *Mus musculus* (BLASTP E value, 8e−05), and although a secretory peptide signal is predicted and a chemokine superfamily domain is detected by the Pfam and Smart databases, no GAG-binding domains or receptor-binding domains were identified.

COTV may represent a novel poxvirus genus. To infer COTV phylogeny, the predicted amino acid sequences of the 90 pro-

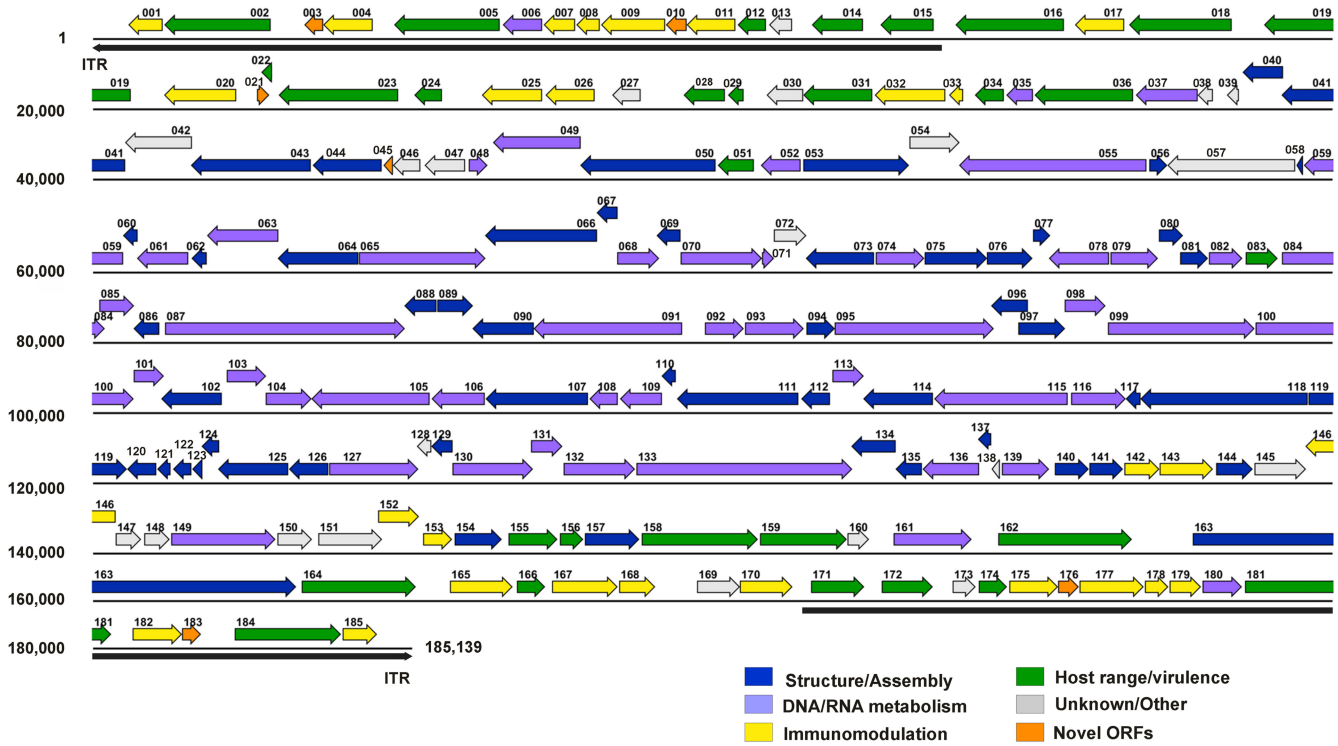

FIG 5 ORF map of the COTV genome. The annotated ORFs are represented by arrows color coded according to their functional categories. The arrows representing ORFs point left or right, indicating the direction of transcription. The inverted terminal repeat (ITR) regions are indicated by long black arrows (shown below the sequence) at the ends of the genome.

teins conserved in all chordopoxviruses were aligned with their respective orthologs from the members of each genus within the *Chordopoxvirinae*. A concatenated alignment was constructed based on the individual alignments, comprising 30,717 amino acids. The overall identity scores of the concatenated sequence were highest with *Cervidpoxvirus* (66.1%), *Capripoxvirus* (65.2%), and *Suipoxvirus* (64.8%), although the individual scores for each protein differed considerably (Table 2). Figure 7 shows phylogenetic trees reconstructed from the concatenated amino acid data sets, using the neighbor-joining (Fig. 7A) and maximum-likelihood (Fig. 7B) methods. We observed that COTV grouped as an independent branch of the *Chordopoxvirinae* supported with high bootstrap values, clearly excluding its classification within established poxvirus genera. Nevertheless, COTV branched within a main clade that included *Capripoxvirus*, *Suipoxvirus*, *Yatapoxvirus*, *Leporipoxvirus*, and *Cervidpoxvirus* (the CSYLC clade) and distant from another chordopoxvirus clade corresponding to the *Orthopoxvirus* genus. Identical topology with high bootstrap value support was also obtained for most parsimony trees (data not shown). Maximum-likelihood distances were estimated for the nucleotide sequences comprising the region limited by VACV orthologs F9L to A34R, and the distances between COTV and cervidpoxviruses, capripoxviruses, and SWPV ranged from 0.869 to 1.088. They were comparable to the distances between distinct genera of the CSYLC clade (0.691 to 1.219) but higher than the estimates for species of the same genus (0.018 to 0.258).

It is noteworthy that several COTV genes related to immunomodulation and virulence were more similar to their *Orthopoxvirus* counterparts than to those in the CSYLC clade (Table 2). Nevertheless, this fact did not alter the clustering of COTV within the CSYLC clade, as determined by the analysis of a phylogeny tree based on the genome nucleotide sequence (data not shown).

In support of the results of the phylogenetic inference, a common genomic feature shared by all members of the CSYLC clade, which is also present in COTV, is worth noting. In this clade, the VACV-Cop C7L homolog (one or more copies in tandem) is inserted between homologs of the VACV-Cop J2R and J3R genes (www.poxvirus.org). COTV has one copy of the C7L homolog (COTV083) in this position, but it also contains a different ortholog of this gene at the 5′-terminal region of the genome (COTV024), unlike other members of the clade (Table 2). In addition, COTV and all clade members, except for DPV, lack orthologs of VACV-Cop A31R and A40R. Similarly, COTV and all CSYLC members but SWPV lack the large subunit of the ribonucleotide reductase (VACV-Cop I4L).

Nevertheless, unlike all members of the CSYLC clade, COTV does not encode a homolog of VACV-Cop B5R, a PHD finger protein, and unlike all CSYLC members except leporipoxviruses, COTV does not encode a G protein-coupled receptor (GPCR) protein (www.poxvirus.org). On the other hand, the COTV genome contains orthologs of VACV-Cop C3L, K1L, and A48R, which are not carried by members of the CSYLC clade (Table 2). Together, these data reinforce the relatedness of COTV to the members of the CSYLC clade but also emphasize the unfeasibility of grouping it within an established genus.

TABLE 2 ORFs encoded by COTV

ORF[a]	Position (bp)	Length (aa)	Best match[b] Species, gene	Length (aa)	% ID[c]	Description/putative function[d]	VACV-Cop ortholog[e]
COTV001	1122-571	183	CPXV-GER1980-EP4, 205	188	32	Serine protease inhibitor-like protein	C13L/C14L
COTV002	2864-1152	570	DPV-W1170-84, 019	643	25	Ankyrin repeat protein	B4R
COTV003	3713-3411	100	*Mustela putorius furo*, gene CCL13	70	35	C-C motif chemokine protein	—
COTV004	4511-3717	264	CPXV-NOR1994-MAN, 002	245	28	Chemokine binding protein	C23L/B29R
COTV005	6560-4860	566	DPV-W848-83, 019	643	25	Ankyrin repeat protein/PRANC domain	B4R
COTV006	7245-6613	210	*Bos taurus*, locus BOS-3916/ CNPV-VR111, 170*	212/212	50/55	Thymidylate kinase	A48R
COTV007	7777-7274	167	CPXV-UK2000-K2984, 003	355	25	TNF receptor-like protein (CrmB)	C22L/B28R
COTV008	8175-7801	124	YKV, 178	127	42	TNF receptor-like protein (CrmE)	—
COTV009	9230-8199	343	MPXV-ZAR-1979, 005/187	354	37	Soluble IFN-α/β receptor	B19R
COTV010	9577-9245	110	*Mus musculus*, gene Scya2	148	25	C-C motif chemokine protein	—
COTV011	10363-9581	260	CPXV-GER91, 001/219	252	26	C-C chemokine binding protein (35-kDa major secreted virus protein)	B29R
COTV012	10856-10404	150	LSDV-LW1959, 001/161	159	47	NF-κB inhibitor/virulence factor	B15R
COTV013	11278-10910	122	RFV-Kas, 004/163	125	49	Unknown	—
COTV014	12422-11601	273	CPXV-UK2000-K2984, 009	273	31	Kelch-like protein	A55R
COTV015	13562-12708	284	ECTV-Mos, 004	273	29	Kelch-like protein	A55R
COTV016	15664-13919	581	MYXV-Lau, 152	675	24	Ankyrin repeat protein	—
COTV017	16637-15846	263	DPV-W1170-84, 010	272	35	Soluble IFN-γ receptor	B8R
COTV018	18372-16720	550	LSDV-NW-LW, 148	550	24	Kelch-like protein	F3L
COTV019	20606-18897	569	YMTV-Amano, 007	637	26	Ankyrin repeat protein/PRANC domain	B4R
COTV020	22308-21148	386	VACV-Cop, 254	353	36	Soluble IFN-α/β-receptor	B19R
COTV021	22645-22839	64	—	—	—	Hypothetical protein	—
COTV022	22886-22716	56	VARV-BEN68-59, 008	58	76	Ankyrin repeat protein/orthopoxvirus C10L protein	WR-018
COTV023	24921-22996	641	CPXV-BR, 027	632	62	Ankyrin repeat protein	C9L
COTV024	25628-25185	147	VACV-WR, 021	150	56	Host range virulence factor	C7L
COTV025	27243-26275	322	CPXV-FIN2000-MAN, 031	321	68	IL-1 receptor antagonist	C10L/C4L
COTV026	28091-27303	262	CPXV-UK2000-K2984, 032	262	65	Complement binding protein	C3L
COTV027	28833-28378	151	CPXV-GER1990-2, 036	176	70	Alpha-amanitin sensitivity protein	N2L
COTV028	30193-29531	220	CPXV-NOR1994-MAN, 038	220	72	NF-κB inhibitor	M2L
COTV029	30495-30247	82	CPXV-NOR1994-MAN, 041	88	64	IFN resistance/eIF2α-like PKR inhibitor	K3L
COTV030	31457-30870	195	AMEV-Moyer, 173‡	209	23	Hypothetical protein	—
COTV031	32571-31462	369	VACV-GLV-1h68, 037	284	27	Ankyrin repeat protein/host range protein/NF-κB and PKR inhibitor	K1L
COTV032	33750-32614	378	DPV-W848-83, 018	382	42	Serine protease inhibitor-like (SPI-3)/ fusion regulatory protein	K2L
COTV033	34038-33814	74	*Anopheles darlingi*, locus AND-04657/SPPV-A, 013	241/100	43/34	Epidermal growth factor-like domain	C11R
COTV034	34694-34230	154	YMTV-Amano, 011	172	28	Apoptosis inhibitor	F1L
COTV035	35163-34738	141	MYXV-Lau, 016	148	64	dUTPase	F2L
COTV036	36780-35194	528	DPV-W848-83, 025	529	34	Kelch-like protein	F3L
COTV037	37822-36827	331	DPV-W848-83, 026	321	74	Ribonucleotide reductase small subunit	F4L
COTV038	38067-37825	80	SPPV-TU, 018‡	79	34	Hypothetical protein	—
COTV039	38487-38296	63	YLDV-Davis, 024	50	68	Unknown	F8L
COTV040	39200-38550	216	DPV-W848-83, 030	215	56	S-S bond formation pathway protein	F9L
COTV041	40515-39178	445	SWPV-Neb, 022	440	76	Serine/threonine kinase	F10L
COTV042	41592-40516	358	DPV-W1170-84, 032	381	40	RhoA inhibitor/cell motility	F11L
COTV043	43510-41579	643	DPV-W1170-84, 033	651	45	WV-associated protein	F12L
COTV044	44654-43545	369	DPV-W848-83, 034	375	69	Palmitylated EV envelope protein	F13L
COTV045	44835-44686	49	—	—	—	Hypothetical protein	—
COTV046	45278-44838	146	DPV-W848-83, 036	148	56	Unknown	F15L
COTV047	46000-45350	216	SWPV-Neb, 028	217	36	Unknown	F16L
COTV048	46060-46359	99	YMTV-Amano, 025	104	74	Nucleic acid binding phosphoprotein	F17R
COTV049	47865-46453	470	SPPV-TU, 029	474	74	Poly(A) polymerase large subunit	E1L
COTV050	50042-47862	726	SWPV-Neb, 031	732	54	WV assembly/interaction with F12	E2L
COTV051	50659-50081	192	SPPV-TU, 031	177	43	IFN resistance/dsRNA-binding protein/ PKR inhibitor	E3L

(Continued on following page)

TABLE 2 (Continued)

ORF[a]	Position (bp)	Length (aa)	Best match[b] Species, gene	Length (aa)	% ID[c]	Description/putative function[d]	VACV-Cop ortholog[e]
COTV052	51414-50776	212	RFV-Kas, 035	222	60	RNA polymerase 30-kDa subunit	E4L
COTV053	51458-53161	567	DPV-W848-83, 044	566	70	Core protein/virus morphogenesis	E6R
COTV054	53171-53977	268	DPV-W848-83, 045	267	80	Unknown	E8R
COTV055	56994-53974	1006	LSDV-LW1959, 041	1006	70	DNA polymerase	E9L
COTV056	57041-57328	95	RFV-Kas, 040	96	76	Sulfhydryl oxidase	E10R
COTV057	59394-57337	685	DPV-W1170-84, 048	678	41	Unknown	O1L
COTV058	59521-59417	34	MYXV-Lau, 042	32	68	MV entry-fusion complex	O3L
COTV059	60481-59537	314	DPV-W848-83, 049	313	69	DNA-binding protein	I1L
COTV060	60715-60482	77	SWPV-Neb, 040	75	56	Virus assembly, crescent formation	I2L
COTV061	61532-60708	274	DPV-W848-83, 051	272	60	DNA-binding phosphoprotein	I3L
COTV062	61830-61588	80	DPV-W848-83, 053	78	39	MV membrane protein	I5L
COTV063	62986-61838	382	DPV-W848-83, 054	389	59	Telomere binding protein	I6L
COTV064	64277-62979	432	DPV-W848-83, 055	432	76	Virion core protease	I7L
COTV065	64287-66326	679	LSDV-LW1959, 051	683	67	RNA helicase/NPH-II	I8R
COTV066	68128-66323	601	SWPV-Neb, 047	593	63	Metalloprotease	G1L
COTV067	68460-68125	111	MYXV-Lau, 051	111	51	MV entry-fusion complex	G3L
COTV068	68454-69128	224	SPPV-TU, 049	222	52	Viral late transcription elongation factor	G2R
COTV069	69475-69092	127	SPPV-TU, 050	126	78	Glutaredoxin protein	G4L
COTV070	69478-70788	436	DPV-W1170-84, 061	434	55	Flap endonucleases (FEN-1)	G5R
COTV071	70791-70982	63	LSDV-Nee, 056	63	79	RNA polymerase subunit RPO7	G5.5R
COTV072	70982-71503	173	RFV-Kas, 056	174	63	NlpC/P60 superfamily	G6R
COTV073	72597-71500	365	DPV-W848-83, 064	375	60	Assembly/seven-protein complex	G7L
COTV074	72627-73406	259	LSDV-Nee, 059	260	81	Viral late transcription factor VLTF-1	G8R
COTV075	73416-74420	334	DPV-W1170-84, 066	335	61	MV entry-fusion complex	G9R
COTV076	74421-75152	243	DPV-W1170-84, 067	249	79	Myristylated MV membrane protein	L1R
COTV077	75164-75439	91	DPV-W848-83, 068	95	46	Virus assembly, crescent formation	L2R
COTV078	76390-75422	322	LSDV-Nee, 063	318	72	Core protein, early transcription	L3L
COTV079	76415-77176	253	DPV-W848-83, 070	252	80	DNA-binding virion protein VP8	L4R
COTV080	77195-77581	128	SPPV-TU, 061	132	56	MV entry-fusion complex	L5R
COTV081	77538-77984	148	LSDV-LW1959, 067	148	72	Assembly/seven-protein complex	J1R
COTV082	78003-78539	178	SWPV-Neb, 063	180	68	Thymidine kinase	J2R
COTV083	78596-79108	170	YLDV-Davis, 069	178	43	Host range virulence factor	C7L
COTV084	79181-80182	333	DPV-W1170-84, 075	374	76	Poly(A) polymerase small subunit	J3R
COTV085	80097-80654	185	SWPV-Neb, 066	185	75	RNA polymerase subunit RPO22	J4R
COTV086	81064-80651	137	SWPV-Neb, 067	134	59	MV entry-fusion complex	J5L
COTV087	81158-85024	1288	DPV-W1170-84, 078	1286	82	RNA polymerase subunit RPO147	J6R
COTV088	85536-85021	171	DPV-W1170-84, 079	172	80	Serine/tyrosine dual phosphatase	H1L
COTV089	85551-86123	190	DPV-W1170-84, 080	190	67	MV entry-fusion complex	H2R
COTV090	87106-86120	328	SWPV-Neb, 071	324	56	MV heparin binding surface protein	H3L
COTV091	89500-87107	797	SWPV-Neb, 072	801	75	RNA polymerase-associated protein RAP94	H4L
COTV092	89869-90492	207	SWPV-Neb, 073	181	41	Viral late transcription factor VLTF-4	H5R
COTV093	90516-91460	314	SWPV-Neb, 074	320	68	DNA topoisomerase type I	H6R
COTV094	91507-91962	151	SWPV-Neb, 075	149	55	Virus assembly, crescent formation	H7R
COTV095	91963-94527	854	DPV-W848-83, 086	843	70	Capping enzyme large subunit	D1R
COTV096	95079-94489	196	SWPV-Neb, 077	146	45	Assembly/seven-protein complex	D2L
COTV097	94925-95677	250	SWPV-Neb, 078	244	41	Assembly/seven-protein complex	D3R
COTV098	95674-96330	218	DPV-W848-83, 089	218	78	Uracil DNA glycosylase	D4R
COTV099	96372-98735	787	DPV-W1170-84, 090	786	69	DNA-independent NTPase	D5R
COTV100	98755-100647	630	LSDV-Nee, 085	635	86	Viral early transcription factor (VETF) small subunit	D6R
COTV101	100650-101135	161	SWPV-Neb, 082	161	81	RNA polymerase subunit RPO18	D7R
COTV102	102071-101097	324	MYXV-Lau, 088	286	31	Carbonic anhydrase-like protein	D8L
COTV103	102152-102784	210	DPV-W848-83, 093	211	59	Decapping enzyme/Nudix hydrolase motif	D9R
COTV104	102781-103518	245	TANV-KEN, 091	255	58	Decapping enzyme/Nudix hydrolase motif	D10R
COTV105	105424-103520	634	DPV-W1170-84, 095	635	72	NPH-I; transcription elongation, termination, release factor	D11L
COTV106	106314-105460	284	SWPV-Neb, 086	287	73	Capping enzyme, small subunit	D12L

(Continued on following page)

TABLE 2 (Continued)

ORF[a]	Position (bp)	Length (aa)	Best match[b] Species, gene	Length (aa)	% ID[c]	Description/putative function[d]	VACV-Cop ortholog[e]
COTV107	107980-106331	549	DPV-W848-83, 097	550	80	Crescent/IV scaffold protein; rifampin resistance	D13L
COTV108	108460-108008	150	DPV-W848-83, 098	151	64	Viral late transcription factor VLTF-2	A1L
COTV109	109173-108499	224	MYXV-Lau, 095	224	87	Viral late transcription factor VLTF-3	A2L
COTV110	109397-109170	75	MYXV-Lau, 096	75	68	Thioredoxin-like protein	A2.5L
COTV111	111374-109419	651	SWPV-Neb, 091	652	76	Core wall protein	A3L
COTV112	111885-111424	153	DPV-W1170-84, 102	151	42	Core wall protein	A4L
COTV113	111925-112428	167	YMTV-Amano, 089	165	57	RNA polymerase subunit RPO19	A5R
COTV114	113546-112425	373	DPV-W848-83, 104	374	74	Virion morphogenesis	A6L
COTV115	115720-113570	716	DPV-W1170-84, 105	715	78	Viral early transcription factor (VETF) large subunit	A7L
COTV116	115777-116555	292	MYXV-Lau, 102	286	66	Viral intermediate transcription factor VITF-3	A8R
COTV117	116896-116660	78	DPV-W1170-84, 107	81	76	MV membrane protein	A9L
COTV118	119593-116897	898	DPV-W1170-84, 108	915	64	Core wall protein	A10L
COTV119	119608-120537	309	RFV-Kas, 105	314	69	Virus assembly, crescent formation	A11R
COTV120	121013-120546	155	YMTV-Amano, 096	167	61	Core structural protein	A12L
COTV121	121243-121031	70	LSDV-Nee, 105	67	47	MV maturation protein	A13L
COTV122	121579-121286	97	MYXV-Lau, 108	96	52	MV membrane protein	A14L
COTV123	121757-121596	53	LSDV-Nee, 107	53	79	MV membrane protein, virulence factor	A14.5L
COTV124	122028-121747	93	DPV-W848-83, 114	94	57	Assembly/seven-protein complex	A15L
COTV125	123142-122012	376	DPV-W848-83, 115	380	60	MV entry-fusion complex	A16L
COTV126	123789-123157	210	DPV-W848-83, 116	197	57	MV membrane protein	A17L
COTV127	123804-125240	478	DPV-W1170-84, 117	482	60	DNA helicase, transcription elongation factor	A18R
COTV128	125451-125221	76	DPV-W848-83, 118	75	66	Unknown	A19L
COTV129	125795-125454	113	DPV-W848-83, 119	115	61	MV entry-fusion complex	A21L
COTV130	125794-127089	431	DPV-W1170-84, 120	428	51	DNA polymerase processivity factor	A20R
COTV131	127061-127564	167	DPV-W848-83, 121	181	79	Holliday junction resolvase	A22R
COTV132	127587-128735	382	RFV-Kas, 118	385	59	Viral intermediate transcription factor VITF-3	A23R
COTV133	128762-132241	1159	DPV-W1170-84, 123	1155	83	RNA polymerase subunit RPO132	A24R
COTV134	132944-132231	237	DPV-W848-83, 124	137	45	MV attachment protein	A27L
COTV135	133367-132945	140	DPV-W848-83, 125	140	69	MV entry-fusion complex	A28L
COTV136	134290-133382	302	DPV-W848-83, 126	300	64	RNA polymerase subunit RPO35	A29L
COTV137	134486-134274	70	DPV-W848-83, 127	75	67	Assembly/seven-protein complex	A30L
COTV138	134625-134494	43	LSDV-Nee, 122‡	41	44	Hypothetical protein	—
COTV139	134659-135417	252	DPV-W848-83, 129	254	82	DNA packaging protein	A32L
COTV140	135513-136058	181	CMLV-M96, 154	184	33	EV envelope glycoprotein	A33R
COTV141	136071-136610	179	SWPV-Neb, 121	169	37	EV envelope glycoprotein	A34R
COTV142	136636-137196	186	SWPV-Neb, 122	185	42	MHC class II inhibitor	A35R
COTV143	137204-138061	285	SWPV-Neb, 123	314	30	Concanavalin-like precursor	—
COTV144	138116-138703	195	SWPV-Neb, 124‡	199	26	WV transmembrane phosphoprotein	A36R
COTV145	138735-139562	275	SWPV-Neb, 125	280	40	Unknown	A37R
COTV146	140356-139559	265	MYXV-Lau, 133	299	29	CD47-like protein	A38L
COTV147	140358-140765	135	DPV-W1170-84, 137	138	39	Unknown	E7R
COTV148	140819-141226	135	SPPV-TU, 129	161	47	Superoxide dismutase-like protein	A45R
COTV149	141254-142933	559	DPV-W848-83, 143	562	58	DNA ligase	A50R
COTV150	142968-143522	184	DPV-W848-83, 146	188	37	Unknown	—
COTV151	143628-144653	341	SPPV-TU, 134	335	36	Unknown	A51R
COTV152	144592-145248	218	MYXV-Lau, 144	192	45	Toll/IL-1-receptor protein	A52R
COTV153	145319-145783	154	LSDV-Nee, 138	186	32	Ig domain OX-2-like protein	A56R
COTV154	145827-146585	252	YLDV-Davis, 145	309	62	Serine/threonine kinase	B1R
COTV155	146697-147482	261	MYXV-Lau, 148	234	35	Ubiquitin ligase/host defense modulator	—
COTV156	147526-147900	124	MYXV-SG33, 150	138	42	Apoptosis inhibitor/NF-κB inhibitor	N1L
COTV157	147929-148804	291	SPPV-TU, 140	302	39	Tyrosine kinase-like protein	—
COTV158	148846-150717	623	DPV-W848-83, 159	641	38	Ankyrin repeat protein/PRANC domain	B4R
COTV159	150755-152152	465	LSDV-Nee, 150	447	25	Ankyrin repeat protein	—
COTV160	152167-152511	114	DPV-W1170-84, 166	94	39	Unknown	—

(Continued on following page)

TABLE 2 (Continued)

ORF[a]	Position (bp)	Length (aa)	Best match[b] Species, gene	Length (aa)	% ID[c]	Description/putative function[d]	VACV-Cop ortholog[e]
COTV161	152910-154166	418	CPXV-GER91, 042	424	51	Phospholipase-D-like protein/nicking-joining enzyme	K4L
COTV162	154599-156752	717	MYXV-Lau, 152	675	21	Ankyrin repeat protein	B4R
COTV163	157738-163266	1842	CPXV-AUS1999-867, 206	1924	57	Surface glycoprotein	—
COTV164	163359-165197	612	LSDV-LW1959, 150	636	25	Ankyrin repeat protein/PRANC domain	—
COTV165	165751-166758	335	CPXV-GER91-3, 195	346	55	Serine protease inhibitor (SPI-2/CrmA)	B13R/B14R
COTV166	166831-167283	150	CPXV-GER91-3, 196	149	65	NF-κB inhibitor/virulence factor	B15R
COTV167	167398-168453	351	CPXV-AUS1999-867, 204	373	57	Serine protease inhibitor-like SPI-1	C12L
COTV168	168481-169059	192	CPXV-BR, 014	202	42	TNF-like receptor protein (CrmB)	C22L/B28R
COTV169	169738-170427	229	DPV-W1170-84, 009	244	45	Alpha-amanitin sensitivity protein	N2L
COTV170	170429-171274	281	*Leopardus pardalis*, gene FLA-I/SQPV-I2L*	338/344	26/22	MHC class I antigen	—
COTV171	171578-172432	284	ECTV-Mos, 004	273	29	Kelch-like protein	A55R
COTV172	172718-173539	273	CPXV-UK2000-K2984, 009	273	31	Kelch-like protein	A55R
COTV173	173862-174230	122	RFV-Kas, 004/163	125	49	Unknown	—
COTV174	174284-174736	150	LSDV-LW1959, 001/161	159	47	NF-κB inhibitor/virulence factor	B15R
COTV175	174777-175559	260	CPXV-GER91, 001/219	252	26	C-C chemokine binding protein (35-kDa major secreted virus protein)	B29R
COTV176	175563-175895	110	*Mus musculus*, gene Scya2	148	25	C-C motif chemokine protein	—
COTV177	175910-176941	343	MPXV-ZAR-1979, 005/187	354	37	Soluble IFNα/β receptor	B19R
COTV178	176965-177339	124	YKV, 178	127	42	TNF receptor-like protein (CrmE)	—
COTV179	177363-177866	167	CPXV-UK2000-K2984, 003	355	25	TNF receptor-like protein (CrmB)	C22L/B28R
COTV180	177895-178527	210	*Bos taurus*, locus BOS_3916/CNPV-VR111, 170*	212/212	55/50	Thymidylate kinase	A48R
COTV181	178580-180280	566	DPV-W848-83, 019	643	25	Ankyrin repeat protein/PRANC domain	B4R
COTV182	180629-181423	264	CPXV-NOR1994-MAN, 002	245	28	Chemokine binding protein	C23L/B29R
COTV183	181427-181729	100	*Mustela putorius furo*, gene CCL13	70	35	C-C motif chemokine protein	—
COTV184	182276-183988	570	DPV-W1170-84, 019	643	25	Ankyrin repeat protein	B4R
COTV185	184018-184569	183	CPXV-GER1980-EP4, 205	188	32	Serine protease inhibitor -like protein	C13L/C14L

[a] ORFs in boldface are conserved in all chordopoxviruses and encode proteins used for analysis of phylogeny.
[b] Best-matching protein sequences obtained by BLASTP-NCBI. YKV, Yoka poxvirus; VARV, variola virus; ECTV, ectromelia virus; AMEV, *Amsacta moorei* entomopoxvirus; SPPV, sheeppox virus; TANV, tanapox virus; SQPV, squirrel poxvirus; CMLV, camelpox virus. Symbols: *, the highest score obtained with a cellular protein, but a significant match also with a poxvirus protein, which is indicated after a slash; ‡, no significant match was obtained using BLASTP-NCBI, and scores were obtained by searching the poxvirus database; —, no significant match.
[c] % ID, percentage of amino acid identity.
[d] PRANC, poxvirus protein repeats of ankyrin, C-terminal; TNF, tumor necrosis factor; Crm, cytokine response modifier; IL-1, interleukin-1; eIF2α, α subunit of eukaryotic initiation factor 2; dsRNA, double-stranded RNA; NPH, nucleoside triphosphate phosphohydrolase; NTPase, nucleoside triphosphatase.
[e] —, no VACV-Cop ortholog. In the absence of an ortholog in VACV-Cop, an ortholog in VACV-WR is indicated if available.

DISCUSSION

Novel poxvirus infections have been reported frequently in Brazil (49). Most agents have been characterized as VACV related to the Cantagalo strain (20, 47, 51, 61), whereas others, such as Cotia SPAn232/SAV, have been reported to be related to VACV strain WR (19). Nevertheless, COTV SPAn232 has been studied by different research groups with conflicting results, and its classification has been a matter of discussion (19, 28, 42, 66, 67). In this work, we present a comprehensive study of COTV SPAn232 biology, combining an evaluation of the virus replicative cycle with serologic analyses and high-throughput genome sequencing. Together, these data suggest the classification of COTV as a novel genus within the *Poxviridae*, closely related to *Capripoxvirus*, *Suipoxvirus*, *Yatapoxvirus*, *Leporipoxvirus*, and *Cervidpoxvirus* (the CSYLC clade).

Using a combination of two next-generation sequencing strategies, 454 pyrosequencing and Illumina sequencing, we determined the nucleotide sequence of the 185,139-bp genome. The COTV genome is the largest in the CSYLC clade and has the longest ITRs and the highest A+T content (1, 4, 14, 15, 38, 64, 65). COTV has 185 ORFs and an intriguing assortment of genes related to virulence, host range, and immunomodulation functions. A notable feature of COTV is that nearly 30 of these genes are similar to their *Orthopoxvirus* counterparts, whereas all COTV genes related to essential functions in virus replication/morphogenesis have the highest identity scores with orthologs in the CSYLC clade. Actually, some of these COTV ORFs related to host interaction do not have orthologs in the CSYLC clade, and until now, genes such as C3L and K1L were considered unique to the genus *Orthopoxvirus* (www.poxvirus.org).

C3L encodes a secreted virus complement control protein (VCP), which is also located on the cell surface. VCP has four SCR domains, binds C3b and C4b, and plays a major role in inhibiting complement-mediated neutralization of orthopoxviruses during infection (29, 35, 36). The VCP homolog in COTV (COTV026) is predicted to be secreted and has the four SCR domains necessary for its function. K1L, in turn, encodes an ankyrin repeat protein, which is an inhibitor of NF-κB and PKR activation during VACV

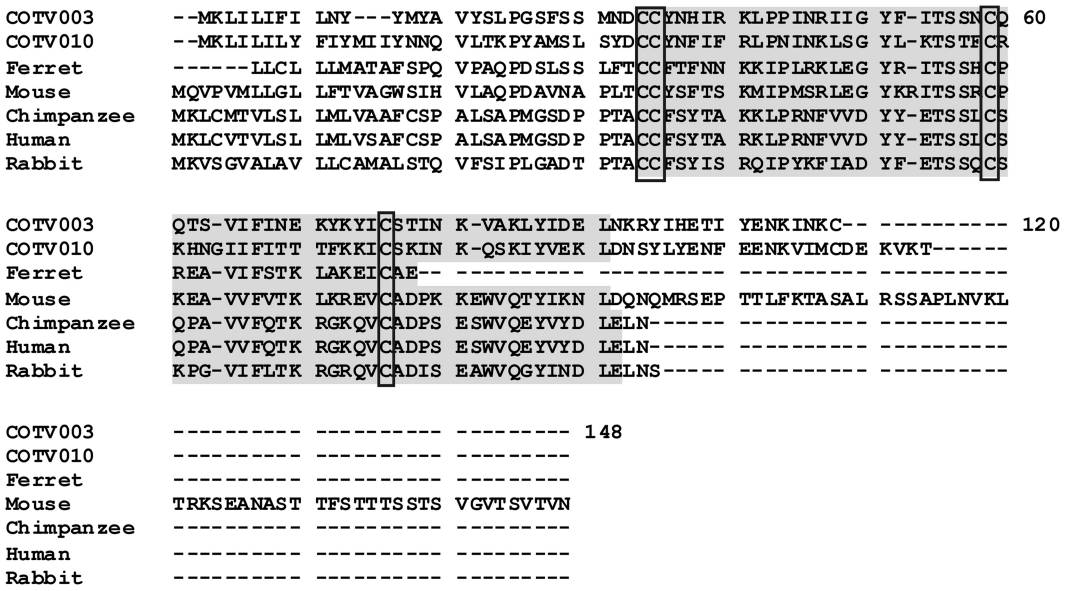

FIG 6 Amino acid alignment of COTV C-C motif chemokine-like proteins (COTV003 and COTV010) with cellular homologs. The chemokine superfamily domain detected by Pfam, Smart, and InterPro is shaded. The four conserved cysteine residues involved in the formation of two disulfide bonds are boxed. Amino acid positions are indicated on the right. GenBank accession numbers are as follows: *Mustela putorius furo* (ferret) C-C motif chemokine ligand 13, ACJ54430.1; *Mus musculus* (mouse) small inducible cytokine A2 precursor, AAF15379.1; *Pan troglodytes* (chimpanzee) C-C motif chemokine 4 isoform 3, XP_001173914; *Homo sapiens* (human) Act-2 cytokine, AAB00790; *Oryctolagus cuniculus* (rabbit) C-C motif chemokine ligand 3-like, XP_002719292.

infection (57, 68). K1 is a host range protein essential for VACV replication in human cells. However, in the absence of K1 expression, the product of the VACV host range gene C7L can rescue virus replication in human cells but not in rabbit kidney cells (50, 58). COTV031 encodes an ortholog of VACV-Cop K1L with predicted ankyrin repeat domains, which is likely to be functional. Unlike K1L, which was considered unique to *Orthopoxvirus* until now, C7L has orthologs in both *Orthopoxvirus* and the CSYLC clade, but in different genomic locations (www.poxvirus.org). In COTV, there are two distinct C7L orthologs. COTV083 is located between the thymidine kinase gene (COTV082) and the small subunit of the poly(A) polymerase gene (COTV084), as in all members of the CSYLC clade. The highest identity score matches YLDV-Davis gene 069. Nevertheless, the other C7L ortholog (COTV024) is located at the 5′ end of the genome, as in all members of the genus *Orthopoxvirus*, but in contrast to members of the CSYLC clade. In this case, the highest identity score matches VACV-WR gene 021.

Taken together, these intriguing features allow us to speculate whether COTV could have a wider tropism than other members of the CSYLC clade. These viruses, particularly members of the genera *Capripoxvirus*, *Suipoxvirus*, and *Cervidpoxvirus*, usually have a restricted host range in cell culture compared to that of *Orthopoxvirus* (7, 10, 32, 33, 43, 45). Nonetheless, in support of our assumption, our results show that COTV propagates in a relatively wide range of cell types. In BSC-40 (monkey) and C6 (rat) cells, virus yields increased >100-fold within the first 24 h of infection, as observed by time course analysis of progeny production. Interestingly, discrepant progeny yields were obtained in cells derived from the same species, such as C6 and Rat-2.

Nevertheless, analysis of the complete set of COTV genes is not sufficient to support an inference of its possible natural hosts. In this regard, COTV encodes two completely novel proteins within the *Poxviridae*. COTV003/183 and COTV010/176 encode C-C chemokine-like proteins similar to homologs in ferret and mouse, respectively. In addition, COTV also encodes an MHC class I heavy chain protein (COTV170), which is more similar to the MHC-I homolog of *Leopardus pardalis* (BLASTP E value, 2e−18) than to those of squirrelpox virus (SQPV) (E value, 7e−17) and MOCV (E value, 1e−12). Interestingly, *L. pardalis* is a wild cat typical of the neotropical forests of South and Central America. Although these three genes are thought to have been acquired from vertebrate hosts, the discrepant origins do not allow any further inference. Even so, the presence of two novel C-C chemokine-like genes in the genome highlights an important role of this pathway in COTV pathogenesis. This is particularly evident because COTV also encodes four poxvirus-like C-C chemokine-binding proteins. The chemokine network regulates several immune and inflammatory functions in vertebrates, such as cell recruitment, angiogenesis, and T-cell differentiation (13). Poxviruses have developed strategies to modulate this pathway, but only MOCV, *Avipoxvirus*, and COTV encode C-C chemokine-like proteins, although they do not share significant identity levels (3, 55, 63).

Despite the presence of virulence/immunomodulatory genes with high identity to orthologs in *Orthopoxvirus*, COTV is clearly less cytopathic than orthopoxviruses, developing noncytolytic patterns of infection similar to those of members of the CSYLC clade (8, 43, 48). Cells infected with COTV induced moderate inhibition of host translation and generated CPE much later than did VACV infection. In addition, COTV-induced CPE started at different times postinfection in BSC-40 and C6 cells, despite similar kinetics of virus production and gene expression. These results may suggest distinct interactions with host proteins involved in the process of cellular morphological changes during COTV infection. Indeed, different patterns of cytoskeleton rearrangement

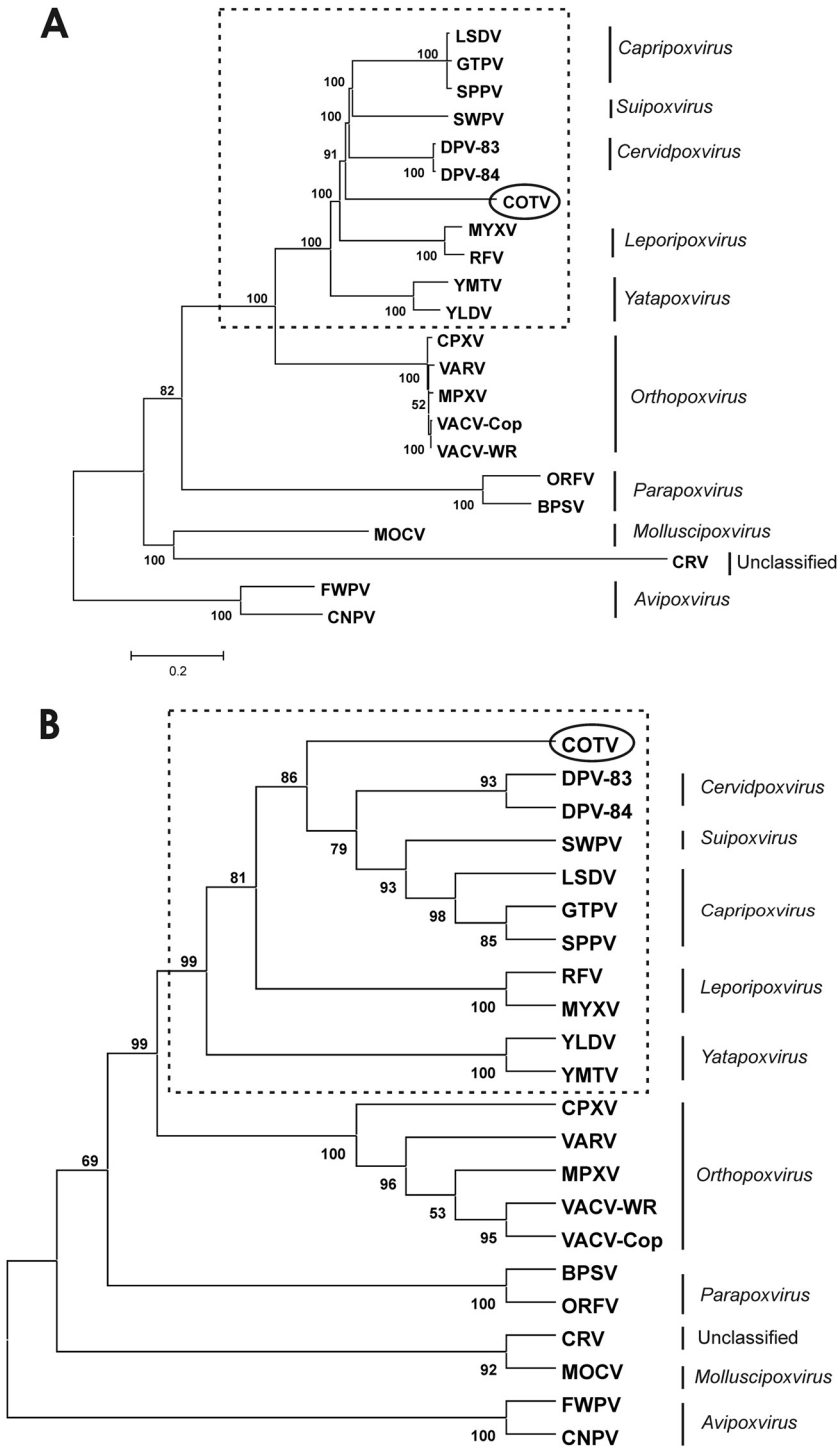

FIG 7 Phylogenetic inference of COTV. The concatenated data set was obtained by combining the individual alignments of the predicted amino acid sequences for 90 genes conserved in 22 chordopoxviruses (ORFs in boldface in Table 2). The combined alignment was used to construct the neighbor-joining tree, opting for the JTT model of substitution, with 2,500 bootstrap replicates, using MEGA 4 (A), and the maximum-likelihood tree, opting for WAG correction for multiple substitutions, 10,000 quartet puzzling steps, and the gamma heterogeneity model (B). The bar in panel A represents relative genetic distance. The poxvirus genera and subfamilies are given on the right. Dashed boxes enclose the poxvirus CSYLC clade, which includes *Capripoxvirus*, *Suipoxvirus*, *Yatapoxvirus*, *Leporipoxvirus*, and *Cervidpoxvirus*.

seem to occur in BSC-40- and C6-infected cells, and this issue is currently being investigated in detail (P. P. Afonso, C. Mermelstein, N. Cunha-e-Silva, and C. R. Damaso, unpublished data).

In addition, COTV produced tiny virus plaques only after 8 days of infection, suggesting a deficient mechanism of cell-to-cell spread compared to that of VACV. A notable feature of COTV that may be involved in this process is the lack of an ortholog of VACV-Cop B5R, which is present in all orthopoxviruses and in all

members of the CSYLC clade. B5 is an EV membrane glycoprotein with four SCR domains. Together with A33, A34, A36, F12, F13, and E2, B5 plays an important role in the wrapping of MV through the *trans*-Golgi network or late endosomes to generate WV, as well in the production of EV, responsible for the cell-to-cell spread of infection (26, 53). In the absence of B5 expression, VACV forms less WV and EV, small plaques, and few actin tails, reducing virus spread (26, 69). Interestingly, despite the absence of an ortholog of B5R in COTV, we consistently detected WV and EV in infected cells by transmission electron microscopy. In addition, studies in progress in our laboratory show that COTV induces the formation of actin tails. Their involvement in the spread of virus infection in BSC-40 and C6 cells is currently being addressed (Afonso et al., unpublished). As mentioned above, it is also interesting that, unlike all members of the CSYLC clade, COTV encodes an ortholog of VACV C3L (COTV026), which, like B5R, encodes a protein containing four SCR domains. These domains in B5 are important for the formation of actin tails during VACV infection (44). Nevertheless, C3 does not replace B5 in *Orthopoxvirus* (26, 69). Whether the COTV ortholog of C3 could somehow participate in the process of virus release and spread has yet to be investigated.

Our phylogenetic inferences support the suggestion that COTV represents a novel genus within the CSYLC clade and is therefore distant from the *Orthopoxvirus* clade. Previous work from Ueda's and Esposito's laboratories had hypothesized that COTV could be a member of a novel poxvirus genus (28, 66, 67). Consistent with their findings, we did not observe significant cross-reaction or cross-neutralization of an anti-COTV antiserum with VACV, MYXV, or SWPV proteins. In addition, COTV orthologs of VACV J2R and G1L were 100% identical to those present in Ueda's (67) and Damon's (40) samples, respectively (the latter was the same sample used by Esposito's group at the CDC, Atlanta, GA). The results presented here particularly conflict with a previous report characterizing COTV SPAn232 as a VACV strain named SAV, closely related to VACV-WR (17). This noticeable divergence of data could be related to the possible presence of VACV in the COTV sample of Kroon's group (62). In this case, the selection of VACV plaques during the plaque purification procedure would have been favored because VACV plaques appear much earlier than COTV plaques, as shown here. Nevertheless, the hypothesis of COTV and VACV coinfection was ruled out for the samples sent to our laboratory. The original brain extracts of mice, as well as all COTV passages up to the last cycle of virus plaque purification, were tested by PCR and found positive for detection of the COTV TK gene but negative for amplification of the *Orthopoxvirus* hemagglutinin (HA) gene, even in seminested PCR assays (data not shown).

It is interesting to speculate about COTV infection in nature. Reisolation has not been reported following the initial virus isolation in the 1960s. Therefore, there is no evidence suggestive of COTV circulation in Brazil, although we cannot exclude the possibility of asymptomatic hosts carrying the virus in the wild. Serological and molecular surveys in Cotia field station, São Paulo, Brazil, could shed light on this subject and reveal asymptomatic carriers seropositive for COTV. In sum, we present evidence that COTV may represent a member of a new genus with a unique set of genes devoted to host range, virulence, and immunomodulatory functions. This study opens up the possibility of uncovering novel and unique biological features of the *Poxviridae*.

ACKNOWLEDGMENTS

We thank Akemi Suzuki, Luiz Eloy Pereira, Terezinha Lisieux Coimbra, and Marli Ueda (Instituto Adolfo Lutz, São Paulo, Brazil) for providing COTV SPAn232 samples and sharing unpublished data and essential information on COTV history; Richard Moyer and Grant McFadden for virus samples and antiserum; Lilian Ayres for sequencing support at UMG-IBCCF; Thaís Souto-Padrón for the use of the Morgani 268 electron microscope; and the late Ademilson Bizerra for technical assistance.

This work was supported by grants from CNPq, MAPA, INPeTAm, and Faperj to C.R.D. and by grant NIH R01 AI055560 to R.C.C. P.P.A. received fellowships from Faperj and CNPq. P.M.S. and L.C.S. were recipients of fellowships from Capes and Faperj. D.M.J. received a fellowship from CNPq.

REFERENCES

1. **Afonso CL, et al.** 2005. Genome of deerpox virus. J. Virol. **79**:966–977.
2. **Afonso CL, et al.** 2006. Genome of crocodilepox virus. J. Virol. **80**:4978–4991.
3. **Afonso CL, et al.** 2000. The genome of fowlpox virus. J. Virol. **74**:3815–3831.
4. **Afonso CL, et al.** 2002. The genome of swinepox virus. J. Virol. **76**:783–790.
5. **Afonso CL, et al.** 2002. The genome of camelpox virus. Virology **295**:1–9.
6. **Antoine G, Scheiflinger F, Dorner F, Falkner FG.** 1998. The complete genomic sequence of the modified vaccinia Ankara strain: comparison with other orthopoxviruses. Virology **244**:365–396.
7. **Aspden K, Passmore JA, Tiedt F, Williamson AL.** 2003. Evaluation of lumpy skin disease virus, a capripoxvirus, as a replication-deficient vaccine vector. J. Gen. Virol. **84**:1985–1996.
8. **Babiuk S, et al.** 2007. Evaluation of an ovine testis cell line (OA3Ts) for propagation of capripoxvirus isolates and development of an immunostaining technique for viral plaque visualization. J. Vet. Diagn. Invest. **19**:486–491.
9. **Bablanian R.** 1984. Comprehensive virology, vol 19. Poxvirus cytopathogenicity: effects on cellular macromolecular synthesis, p 391–402. Plenum, New York, NY.
10. **Barcena J, Blasco R.** 1998. Recombinant swinepox virus expressing beta-galactosidase: investigation of viral host range and gene expression levels in cell culture. Virology **243**:396–405.
11. **Bawden AL, et al.** 2000. Complete genomic sequence of the *Amsacta moorei* entomopoxvirus: analysis and comparison with other poxviruses. Virology **274**:120–139.
12. **Benson G.** 1999. Tandem repeats finder: a program to analyze DNA sequences. Nucleic Acids Res. **27**:573–580.
13. **Boomker JM, de Leij LF, The TH, Harmsen MC.** 2005. Viral chemokine-modulatory proteins: tools and targets. Cytokine Growth Factor Rev. **16**:91–103.
14. **Brunetti CR, et al.** 2003. Complete genomic sequence and comparative analysis of the tumorigenic poxvirus Yaba monkey tumor virus. J. Virol. **77**:13335–13347.
15. **Cameron C, et al.** 1999. The complete DNA sequence of myxoma virus. Virology **264**:298–318.
16. **Castro AP, Carvalho TM, Moussatche N, Damaso CR.** 2003. Redistribution of cyclophilin A to viral factories during vaccinia virus infection and its incorporation into mature particles. J. Virol. **77**:9052–9068.
17. **Condit RC, Moussatche N, Traktman P.** 2006. In a nutshell: structure and assembly of the vaccinia virion. Adv. Virus Res. **66**:31–124.
18. **Cordeiro JV, et al.** 2009. F11-mediated inhibition of RhoA signalling enhances the spread of vaccinia virus in vitro and in vivo in an intranasal mouse model of infection. PLoS One **4**:e8506.
19. **da Fonseca FG, et al.** 2002. Characterization of a vaccinia-like virus isolated in a Brazilian forest. J. Gen. Virol. **83**:223–228.
20. **Damaso CR, Esposito JJ, Condit RC, Moussatche N.** 2000. An emergent poxvirus from humans and cattle in Rio de Janeiro State: Cantagalo virus may derive from Brazilian smallpox vaccine. Virology **277**:439–449.
21. **Damaso CR, Moussatche N.** 1998. Inhibition of vaccinia virus replication by cyclosporin A analogues correlates with their affinity for cellular cyclophilins. J. Gen. Virol. **79**(Pt 2):339–346.
22. **Damaso CR, Moussatche N.** 1992. Protein synthesis in vaccinia virus-infected cells. I. Effect of hypertonic shock recovery. Arch. Virol. **123**:295–308.

23. **Damaso CR, Oliveira MF, Massarani SM, Moussatche N.** 2002. Azathioprine inhibits vaccinia virus replication in both BSC-40 and RAG cell lines acting on different stages of virus cycle. Virology **300**:79–91.
24. **Drumond BP, et al.** 2008. Brazilian vaccinia virus strains are genetically divergent and differ from the Lister vaccine strain. Microbes Infect. **10**: 185–197.
25. **Edgar RC.** 2004. MUSCLE: a multiple sequence alignment method with reduced time and space complexity. BMC Bioinformatics **5**:113.
26. **Engelstad M, Smith GL.** 1993. The vaccinia virus 42-kDa envelope protein is required for the envelopment and egress of extracellular virus and for virus virulence. Virology **194**:627–637.
27. **Esposito JJ, Fenner F.** 2001. Poxviruses, p 2885–2921. *In* Knipe DM, et al (ed), Fields virology, vol 2. Lippincott Williams & Wilkins, Philadelphia, PA.
28. **Esposito JJ, et al.** 1980. Studies on the poxvirus Cotia. J. Gen. Virol. **47**:37–46.
29. **Girgis NM, et al.** 2008. Cell surface expression of the vaccinia virus complement control protein is mediated by interaction with the viral A56 protein and protects infected cells from complement attack. J. Virol. **82**: 4205–4214.
30. **Gubser C, Hue S, Kellam P, Smith GL.** 2004. Poxvirus genomes: a phylogenetic analysis. J. Gen. Virol. **85**:105–117.
31. **Gubser C, Smith GL.** 2002. The sequence of camelpox virus shows it is most closely related to variola virus, the cause of smallpox. J. Gen. Virol. **83**:855–872.
32. **Hu Y, et al.** 2001. Yaba-like disease virus: an alternative replicating poxvirus vector for cancer gene therapy. J. Virol. **75**:10300–10308.
33. **Johnston JB, Nazarian SH, Natale R, McFadden G.** 2005. Myxoma virus infection of primary human fibroblasts varies with cellular age and is regulated by host interferon responses. Virology **332**:235–248.
34. **Kara PD, et al.** 2003. Comparative sequence analysis of the South African vaccine strain and two virulent field isolates of lumpy skin disease virus. Arch. Virol. **148**:1335–1356.
35. **Kotwal GJ, Isaacs SN, McKenzie R, Frank MM, Moss B.** 1990. Inhibition of the complement cascade by the major secretory protein of vaccinia virus. Science **250**:827–830.
36. **Kotwal GJ, Moss B.** 1988. Vaccinia virus encodes a secretory polypeptide structurally related to complement control proteins. Nature **335**:176–178.
37. **Lassmann T, Sonnhammer EL.** 2005. Kalign—an accurate and fast multiple sequence alignment algorithm. BMC Bioinformatics **6**:298.
38. **Lee HJ, Essani K, Smith GL.** 2001. The genome sequence of Yaba-like disease virus, a yatapoxvirus. Virology **281**:170–192.
39. **Li G, et al.** 2005. Complete coding sequences of the rabbitpox virus genome. J. Gen. Virol. **86**:2969–2977.
40. **Li Y, Meyer H, Zhao H, Damon IK.** 2010. GC content-based pan-pox universal PCR assays for poxvirus detection. J. Clin. Microbiol. **48**:268–276.
41. **Likos AM, et al.** 2005. A tale of two clades: monkeypox viruses. J. Gen. Virol. **86**:2661–2672.
42. **Lopes ODS, et al.** 1965. Cotia virus: a new agent isolated from sentinel mice in São Paulo, Brazil. Am. J. Trop. Med. Hyg. **14**:156–157.
43. **Massung RF, Moyer RW.** 1991. The molecular biology of swinepox virus. II. The infectious cycle. Virology **180**:355–364.
44. **Mathew E, Sanderson CM, Hollinshead M, Smith GL.** 1998. The extracellular domain of vaccinia virus protein B5R affects plaque phenotype, extracellular enveloped virus release, and intracellular actin tail formation. J. Virol. **72**:2429–2438.
45. **McFadden G.** 2005. Poxvirus tropism. Nat. Rev. Microbiol. **3**:201–213.
46. **McInnes CJ, et al.** 2006. Genomic characterization of a novel poxvirus contributing to the decline of the red squirrel (*Sciurus vulgaris*) in the UK. J. Gen. Virol. **87**:2115–2125.
47. **Medaglia ML, Pessoa LC, Sales ER, Freitas TR, Damaso CR.** 2009. Spread of Cantagalo virus to northern Brazil. Emerg. Infect. Dis. **15**:1142–1143.
48. **Mediratta S, Essani K.** 1999. The replication cycle of tanapox virus in owl monkey kidney cells. Can. J. Microbiol. **45**:92–96.
49. **Moussatche N, Damaso CR, McFadden G.** 2008. When good vaccines go wild: feral orthopoxvirus in developing countries and beyond. J. Infect. Dev. Ctries. **2**:156–173.
50. **Perkus ME, et al.** 1990. Vaccinia virus host range genes. Virology **179**: 276–286.
51. **Quixabeira-Santos JC, Medaglia ML, Pescador CA, Damaso CR.** 2011. Animal movement and establishment of vaccinia virus Cantagalo strain in Amazon biome, Brazil. Emerg. Infect. Dis. **17**:726–729.
52. **Rempel RE, Anderson MK, Evans E, Traktman P.** 1990. Temperature-sensitive vaccinia virus mutants identify a gene with an essential role in viral replication. J. Virol. **64**:574–583.
53. **Roberts KL, Smith GL.** 2008. Vaccinia virus morphogenesis and dissemination. Trends Microbiol. **16**:472–479.
54. **Schmidt HA, Strimmer K, Vingron M, von Haeseler A.** 2002. TREE-PUZZLE: maximum likelihood phylogenetic analysis using quartets and parallel computing. Bioinformatics **18**:502–504.
55. **Senkevich TG, et al.** 1996. Genome sequence of a human tumorigenic poxvirus: prediction of specific host response-evasion genes. Science **273**: 813–816.
56. **Shchelkunov SN, et al.** 2000. Alastrim smallpox variola minor virus genome DNA sequences. Virology **266**:361–386.
57. **Shisler JL, Jin XL.** 2004. The vaccinia virus K1L gene product inhibits host NF-κB activation by preventing IκBα degradation. J. Virol. **78**:3553–3560.
58. **Sutter G, Ramsey-Ewing A, Rosales R, Moss B.** 1994. Stable expression of the vaccinia virus K1L gene in rabbit cells complements the host range defect of a vaccinia virus mutant. J. Virol. **68**:4109–4116.
59. **Tamura K, Dudley J, Nei M, Kumar S.** 2007. MEGA4: Molecular Evolutionary Genetics Analysis (MEGA) software version 4.0. Mol. Biol. Evol. **24**:1596–1599.
60. **Thompson JD, Gibson TJ, Plewniak F, Jeanmougin F, Higgins DG.** 1997. The CLUSTAL_X windows interface: flexible strategies for multiple sequence alignment aided by quality analysis tools. Nucleic Acids Res. **25**:4876–4882.
61. **Trindade GDS, et al.** 2003. Aracatuba virus: a vaccinialike virus associated with infection in humans and cattle. Emerg. Infect. Dis. **9**:155–160.
62. **Trindade GS, Emerson GL, Carroll DS, Kroon EG, Damon IK.** 2007. Brazilian vaccinia viruses and their origins. Emerg. Infect. Dis. **13**:965–972.
63. **Tulman ER, et al.** 2004. The genome of canarypox virus. J. Virol. **78**:353–366.
64. **Tulman ER, et al.** 2001. Genome of lumpy skin disease virus. J. Virol. **75**:7122–7130.
65. **Tulman ER, et al.** 2002. The genomes of sheeppox and goatpox viruses. J. Virol. **76**:6054–6061.
66. **Ueda Y, Dumbell KR, Tsuruhara T, Tagaya I.** 1978. Studies on Cotia virus—an unclassified poxvirus. J. Gen. Virol. **40**:263–276.
67. **Ueda Y, Morikawa S, Watanabe T.** 1995. Unclassified poxvirus: characterization and physical mapping of Cotia virus DNA and location of a sequence capable of encoding a thymidine kinase. Virology **210**:67–72.
68. **Willis KL, Patel S, Xiang Y, Shisler JL.** 2009. The effect of the vaccinia K1 protein on the PKR-eIF2α pathway in RK13 and HeLa cells. Virology **394**:73–81.
69. **Wolffe EJ, Isaacs SN, Moss B.** 1993. Deletion of the vaccinia virus B5R gene encoding a 42-kilodalton membrane glycoprotein inhibits extracellular virus envelope formation and dissemination. J. Virol. **67**:4732–4741.
70. **Zerbino DR, Birney E.** 2008. Velvet: algorithms for de novo short read assembly using de Bruijn graphs. Genome Res. **18**:821–829.
71. **Zhao G, et al.** 2011. The genome of Yoka poxvirus. J. Virol. **85**:10230–10238.